MMBR
Journals.ASM.org

Diverse Bacterial Microcompartment Organelles

Chiranjit Chowdhury,[a] Sharmistha Sinha,[a] Sunny Chun,[b] Todd O. Yeates,[b,c,d] Thomas A. Bobik[a]

Roy J. Carver Department of Biochemistry, Biophysics and Molecular Biology, Iowa State University, Ames, Iowa, USA[a]; Molecular Biology Institute,[b] Department of Energy Institute for Genomics and Proteomics,[c] and Department of Chemistry and Biochemistry,[d] University of California, Los Angeles, Los Angeles, California, USA

(continued)

Address correspondence to Thomas A. Bobik, bobik@iastate.edu.

doi:10.1128/MMBR.00009-14

SUMMARY

Bacterial microcompartments (MCPs) are sophisticated protein-based organelles used to optimize metabolic pathways. They consist of metabolic enzymes encapsulated within a protein shell, which creates an ideal environment for catalysis and facilitates the channeling of toxic/volatile intermediates to downstream enzymes. The metabolic processes that require MCPs are diverse and widely distributed and play important roles in global carbon fixation and bacterial pathogenesis. The protein shells of MCPs are thought to selectively control the movement of enzyme cofactors, substrates, and products (including toxic or volatile intermediates) between the MCP interior and the cytoplasm of the cell using both passive electrostatic/steric and dynamic gated mechanisms. Evidence suggests that specialized shell proteins conduct electrons between the cytoplasm and the lumen of the MCP and/or help rebuild damaged iron-sulfur centers in the encapsulated enzymes. The MCP shell is elaborated through a family of small proteins whose structural core is known as a bacterial microcompartment (BMC) domain. BMC domain proteins oligomerize into flat, hexagonally shaped tiles, which assemble into extended protein sheets that form the facets of the shell. Shape complementarity along the edges allows different types of BMC domain proteins to form mixed sheets, while sequence variation provides functional diversification. Recent studies have also revealed targeting sequences that mediate protein encapsulation within MCPs, scaffolding proteins that organize lumen enzymes and the use of private cofactor pools (NAD/H and coenzyme A [HS-CoA]) to facilitate cofactor homeostasis. Although much remains to be learned, our growing understanding of MCPs is providing a basis for bioengineering of protein-based containers for the production of chemicals/pharmaceuticals and for use as molecular delivery vehicles.

INTRODUCTION

Bacterial microcompartments (MCPs) were first observed in the 1950s by electron microscopy (EM) as polyhedral inclusion bodies in the cytoplasm of cyanobacteria (1). The structures seen were about 100 to 200 nm in diameter with a thin protein shell and an electron-dense lumen. Initially, they were thought to be viruses, but later studies with *Thiobacillus* showed that the protein shell was filled with RuBisCO and that these structures play an important role in CO_2 fixation by the Calvin cycle (2). Because of their role in CO_2 fixation, this class of MCPs (which is the archetype of the family) was named the carboxysome (2). Further studies of carboxysome composition paved the way for the identification of diverse MCPs (3). Homologs of carboxysome shell proteins were found in diverse contexts, including operons used for 1,2-propanediol (1,2-PD) and ethanolamine degradation by *Salmonella* (4, 5). Subsequent studies showed that *Salmonella* forms MCPs for the utilization of these compounds as carbon and energy sources (5–8). Today, MCPs are thought to be involved in seven or more metabolic processes (9). All MCPs have related protein shells that are composed primarily of bacterial microcompartment (BMC) domain proteins (10–14). However, different types of MCPs encapsulate different enzymes and have various physiological roles (9, 10, 13–19). The MCPs that have been best studied are similar in overall structure. They are polyhedral, usually about 100 to 150 nm in diameter, and are assembled from about 5 to 20,000 polypeptides of 10 to 20 different types. Studies indicate that MCPs are made completely out of protein subunits, and to date, there is no evidence for lipid components. MCP shells have no detectable structural or sequence relationship to viral capsids. Functionally diverse MCPs are thought to have analogous physiological roles (20).

ESSENTIAL FEATURES OF BACTERIAL MICROCOMPARTMENTS

MCPs Are Used To Optimize Pathways That Have Toxic or Volatile Intermediates

Studies on carboxysomes, ethanolamine utilization (Eut) MCPs, and 1,2-PD utilization (Pdu) MCPs indicate that the general function of bacterial MCPs is to optimize metabolic pathways having

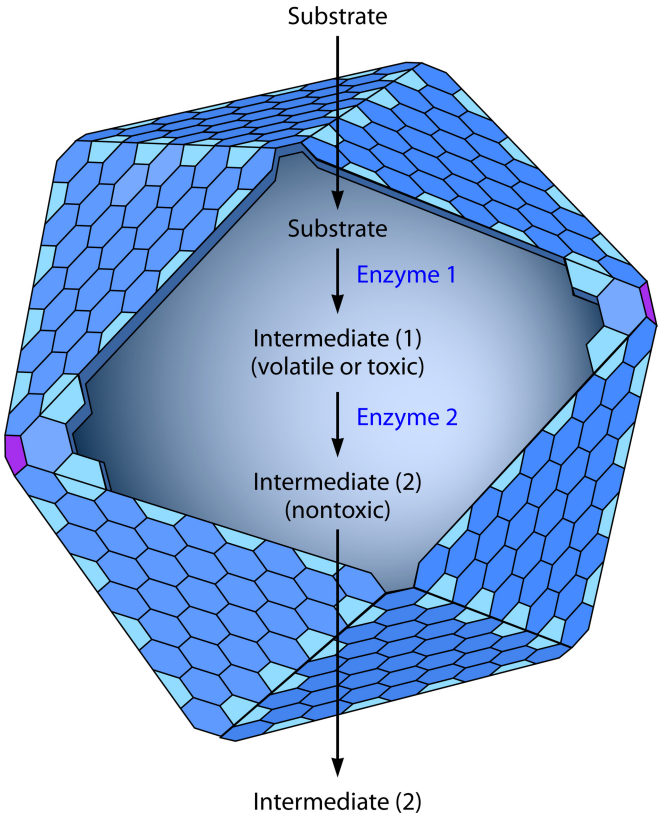

FIG 1 Bacterial microcompartments are used to optimize pathways with toxic or volatile intermediates. The protein shell of the microcompartment acts as a diffusion barrier that helps channel a toxic or volatile intermediate to the next pathway enzyme. In the absence of the microcompartment, such intermediates would either accumulate in the cytoplasm, causing cellular toxicity, or diffuse across the cell envelope and into the environment, resulting in the loss of valuable carbon. The carboxysome and the Pdu and Eut microcompartments help to channel CO_2, propionaldehyde, and acetaldehyde, respectively. All three of these compounds pass easily through the cell envelope, and propionaldehyde and acetaldehyde are cytotoxic. In addition, MCPs may enhance catalysis by bringing enzymes, substrates, and cofactors together at high concentrations.

intermediates that are toxic to the cell or that pass readily through the cell envelope (particularly certain volatile compounds) (2, 21–24). A key feature of MCPs is the use of a protein shell as a diffusion barrier to help channel toxic/volatile metabolic intermediates to downstream enzymes (21–23, 25, 26). A model that outlines how this is achieved is shown in Fig. 1. A metabolic substrate enters a bacterial cell and then diffuses from the cytoplasm into the lumen of the MCP. Within the MCP, the substrate is converted to a toxic or volatile intermediate. The MCP shell acts as a diffusion barrier that helps channel this intermediate to a downstream enzyme, which then converts it to a compound that is nontoxic and/or well retained by the cell envelope. The latter compound moves from the MCP to the cytoplasm, where it enters central metabolism, providing energy and/or carbon for cell growth. In the case of the carboxysome, sequestration allows the concentration of CO_2 to be elevated in the immediate vicinity of RuBisCO, improving its catalytic efficiency (13, 16, 18). For other MCPs, sequestration helps to balance the production and consumption of the toxic/volatile catabolic intermediate. This helps to reduce cytotoxicity, DNA damage, and/or the loss of valuable carbon to the environment (21–23, 26). In addition, the MCP may be used to provide an optimal environment for catalysis by bringing enzymes, substrates, and cofactors together at high concentrations in a precise orientation and possibly by tuning their individual activities.

MCP Distribution and Ecology

Genome sequence analyses indicate that bacterial MCPs are widely distributed and functionally diverse. Current estimates indicate that about 16% of bacteria in 11 different phyla produce MCPs of seven main types, with several subtypes that have extended functionality (9, 20). In addition, recent studies identified a possible eighth type of MCP exclusive to the *Verrucomicrobia* and *Planctomycetes* (27). Multiple MCP types are often found within a single genome, except for carboxysomes, where only one type (α or β) is found per genome (20). Several studies have suggested that MCP loci are subject to frequent horizontal gene transfer, including recent comprehensive analyses of sequenced genomes (6, 13, 20, 28, 29). In many cases, MCPs are encoded by large operons that include multiple MCP shell protein paralogs along with MCP-associated enzymes. The associated enzymes define the MCP type and allow predictions about new MCP functions (9, 15). A number of MCPs have also been investigated experimentally. Studies to date have established that MCPs are used to enhance carbon fixation by the Calvin cycle (the carboxysome) and to optimize the catabolism of 1,2-PD and ethanolamine (the Pdu and Eut MCPs, respectively). In addition, based on sequence analyses, MCPs are predicted to be involved in the metabolism of ethanol, fucose, rhamnose, and an unspecified amino alcohol (9, 20, 27). These compounds are widely found in nature, and their metabolism is important for the natural cycling of matter. Their use provides metabolically capable organisms with a growth advantage in a variety of environments. Of special note is the fact that MCP-dependent processes have a major impact on global carbon fixation and play an important role in the dissemination of enteric pathogens (16, 30).

Carboxysomes Play a Major Role in Global Carbon Fixation

Carboxysomes are found in virtually all bacteria that use the Calvin cycle for CO_2 fixation, including cyanobacteria (a diverse group of photosynthetic bacteria) and many if not all chemoautotrophs (13, 16). Cyanobacteria are widely distributed in freshwater and marine environments, and it has been estimated that as much as 25% of all carbon fixation on Earth occurs within carboxysomes (16). The carboxysome is an essential part of a carbon dioxide-concentrating mechanism (CCM) used to enhance the efficiency of RuBisCO, the rate-limiting enzyme of the Calvin cycle (31). The inefficiency of RuBisCO is due to its relatively low turnover rate (about 1 to 13 s^{-1} depending on the organism) and the fact that it reacts with O_2 in a nonproductive process known as photorespiration, which can drain away up to 50% of the carbon fixed by the Calvin cycle. The bacterial CCM is used to ameliorate these inefficiencies. It begins with active transport processes that elevate the cytoplasmic levels of bicarbonate. Subsequently, bicarbonate is believed to diffuse into the carboxysome, where a carboxysomal carbonic anhydrase (CA) converts HCO_3^- to CO_2 within the carboxysome lumen. The protein shell of the carboxysome restricts the outward diffusion of CO_2, causing it to accumulate proximal to RuBisCO. Elevated CO_2 levels in the immediate vicinity of RuBisCO enhance CO_2 fixation and reduce

competing photorespiration. A key finding that demonstrates the importance of the carboxysome in CO_2 fixation is that cyanobacteria expressing wild-type levels of RuBisCO, but unable to form carboxysomes, are incapable of growth at ambient CO_2 levels. This finding as well as a great deal of additional evidence demonstrating the importance of the CCM in global carbon fixation are described in excellent recent reviews (16, 18); hence, further discussion of the carboxysome here is limited mainly to comparative aspects of MCP function.

The Eut and Pdu MCPs Play Important Roles in Growth and Dissemination of Enteric Pathogens

Recent studies have indicated that ethanolamine degradation, which occurs within the Eut MCP, promotes the growth of *Salmonella* in the inflamed intestine (30). This, in turn, leads to increased transmission of *Salmonella* to new hosts (30). When *Salmonella* colonizes the intestine, it deploys effector molecules that induce an inflammatory response (32). This results in the production of reactive oxygen species that mediate the formation of tetrathionate from thiosulfate (an endogenous sulfur compound) (33). *Salmonella* is then able to respire ethanolamine with tetrathionate as the terminal electron acceptor, which gives it a pronounced growth advantage compared to competing flora (30). Ethanolamine is a particularly important electron donor for tetrathionate respiration because of its prevalence in the intestinal environment (30). Phosphatidylethanolamine is the most abundant lipid in enterocytes, a cell type that is continually shed from the intestinal epithelium.

A number of studies have also suggested that 1,2-PD degradation, which is mediated by the Pdu MCP, is important for enteric pathogenesis. *In vivo* expression studies showed that *pdu* genes are induced in host tissues (34, 35), and competitive index studies with mice showed that *pdu* mutations confer a virulence defect (35). In *Listeria*, comparative genomics indicated a link between 1,2-PD degradation and pathogenesis, and several *pdu* genes are induced during growth within host cells (36, 37). In addition, as described above, recent studies have shown that tetrathionate is an important terminal electron acceptor in the inflamed gut (33), and *Salmonella* is known to respire 1,2-PD with tetrathionate (38). Furthermore, 1,2-PD is expected to be present in the intestinal environment since it is a major product of the anaerobic breakdown of the common plant sugars rhamnose and fucose.

Targeting Systems for Encapsulation of MCP Proteins

For MCPs to function, specific enzymes must be encapsulated within the protein shells. Recent studies have shown that short N-terminal sequences are used to target proteins to diverse MCPs (39–42). The initial hint that targeting sequences are important for the encapsulation of enzymes within MCPs was the observations that the first enzyme of 1,2-PD degradation (the PduCDE diol dehydratase [DDH]) has N-terminal extensions on two of three subunits that were absent from homologs unassociated with MCPs (43) and that these extensions were not required for enzymatic activity (44). Later studies showed that a short C-terminal sequence is used to encapsulate proteins within a compartment, unrelated to MCPs, known as a bacterial nanocompartment (45), and it was suggested that terminal sequences might also be used to target proteins to MCPs, citing prior observations of N-terminal extensions that were nonessential for enzymatic activity (43, 44). Conclusive evidence for MCP targeting sequences was first reported by Fan et al., who showed that a short N-terminal sequence (18 amino acids) was responsible for encapsulation of enzymes into the Pdu MCP (40). A key finding was that deletion of 18 N-terminal amino acids had little effect on the enzymatic activity of PduP but largely prevented its encapsulation into the Pdu MCP (40). In addition, when this 18-amino-acid sequence was fused to green fluorescent protein (GFP), glutathione *S*-transferase (GST), or maltose-binding protein (MBP), these proteins were targeted to the Pdu MCP, proving that this N-terminal sequence was both necessary and sufficient for encapsulation of enzymes into the Pdu MCP (40). Fan et al. also conducted bioinformatic studies that showed that putative N-terminal targeting sequences are widely distributed among diverse MCPs (40). Later studies showed that the predicted targeting sequence of PduD was indeed functional and that it mediated the encapsulation of the PduCDE diol dehydratase into the Pdu MCP (39). In other studies, Choudhary et al. showed that the predicted EutC signal sequence could target proteins to the Eut MCP as well as to recombinant MCP shells (42). In the case of the β-carboxysome, recent studies showed that a short C-terminal sequence of a presumptive scaffolding protein, CcmN, is necessary for MCP assembly (46). Bioinformatic analysis predicted that this sequence (like previously identified N-terminal targeting sequences) forms an amphipathic helix (40, 41). Hence, it was suggested (46) that the C-terminal sequence of CcmN might function in the β-carboxysome similarly to the N-terminal targeting sequences elucidated in previous studies on Pdu and other types of MCPs (40, 46). Additional amphipathic helixes were identified at the C terminus or between domains of several other MCP proteins, suggesting functional conservation (46). With respect to targeting, studies have also shown that heterologous RuBisCO can be localized to the carboxysome (47), that fusions to the entire PduC protein (which lack an identifiable targeting sequence) are directed to the Pdu MCP (48), and that the N-terminal portion of the PduV protein (42 amino acids) mediates the association of heterologous proteins with the exterior of the Pdu MCP (48). It is also of note that a number of MCP-associated enzymes do not have obvious targeting sequences, suggesting that other mechanisms are also used for localization of MCP proteins.

The Mechanism of Protein Targeting to MCPs

Although MCP targeting sequences are reminiscent of plastid signal sequences, their mechanisms and origins are distinctly different. Studies by Fan et al. showed that the N-terminal targeting sequence of the PduP enzyme mediates encapsulation by binding a short C-terminal helix of the PduA or PduJ shell protein (40, 41). This possibility was proposed when N-terminal targeting sequences were first identified (40) and by an analysis of shell protein crystal structures (12). Yeates and colleagues pointed out that the N termini and C termini of shell proteins, which typically reside on the concave side of BMC hexamers, tend to diverge in length and structure between MCP paralogs and often appear flexible or disordered in crystal structures, which are ideal properties for binding sites with divergent specificity. Hence, the finding that lumen enzymes are targeted to MCPs by binding to shell proteins, in conjunction with diverse potential binding sites, led to the proposal that specific lumen enzymes bind partner shell proteins and that this mediates both targeting as well as the internal order of the Pdu MCP (40).

Further studies on the mechanism of enzyme targeting to MCPs were done by using alanine scanning mutagenesis to investigate

the PduP targeting sequence (41). These studies indicated that E7, I10, and L14 of PduP (which are on one face of an α-helix) are the key resides involved in binding the C-terminal helix of the PduA shell protein. Subsequent studies that looked at encapsulation of GFP fused to the PduP targeting sequence found that residues L6, L9, I10, I13, and L14 were most important for encapsulation (49). The differences here may be due to the different methods by which encapsulation was measured: fluorescence microscopy versus MCP purification followed by enzyme assays. More recently, a series of *in vitro* studies were conducted to investigate the targeting of PduP to the Pdu MCP of *Citrobacter freundii* (50). The solution structure of a synthetic peptide corresponding to the PduP targeting sequence was found to be a helix that likely exists in a coiled-coil conformation (50). Further studies indicated that this helix mediated encapsulation by interacting with the PduK shell protein. In contrast, studies conducted with *Salmonella* (described above) indicated that the PduP targeting sequence binds to the PduA and PduJ shell proteins to mediate encapsulation (41). This apparent difference could reflect divergence between the *C. freundii* and *Salmonella* systems, or the PduP targeting sequence might interact with multiple shell proteins. Recent studies of *C. freundii* also indicated that a synthetic 18-amino-acid targeting peptide was capable of diffusing into the lumen of purified empty MCP shells, although surface binding was not ruled out (50). This raises some intriguing questions about the permeability of MCP shells to peptides. Nonetheless, overall, available data support the idea that binding of MCP enzymes to shell proteins results in encapsulation during assembly.

Scaffolding Proteins Are Used To Organize the Interior of the β-Carboxysome

With respect to internal organization, the best-understood MCP is the β-carboxysome (16). In this system, binding studies indicate that the CcmM protein (which has two isoforms) cross-links multiple RuBisCO and carbonic anhydrase (CA) molecules together into an extended network that promotes CO_2 fixation (46, 51–54). The N terminus of CcmM has sequence similarity to γ-CA, and the C terminus typically has three to five tandem repeats with similarity to the small subunit of RuBisCO (SSU-like repeats) (53). In some versions of CcmM, its N-terminal region has redox-sensitive CA activity, while in other versions, CA activity is absent, and an alternative CA (CcaA) is required for carboxysome function. Current models propose that a long form of CcmM (CcmM-58) cross-links RuBisCO, recruits (or provides) carbonic anhydrase activity, and tethers these enzymes to the carboxysome shell (16). Binding to the shell occurs via an intermediary protein (CcmN), which binds to the CcmK2 shell protein via a short C-terminal sequence (46). The short form of CcmM (CcmM-35) consists only of SSU-like repeats and is proposed to be restricted to the central portion of the carboxysome (away from the shell), where it further cross-links RuBisCO. Currently, only the β-carboxysome has been shown to have extensive internal organization. Further studies are needed to understand the primary factors that control the internal organization of other MCPs.

MCP Assembly

MCP assembly has been studied primarily for the carboxysome. Recent work with the β-carboxysome of *Synechococcus* indicates that the cargo proteins (RuBisCO and CA) assemble into a procarboxysome by a process that requires CcmM (55, 56). Subsequently or concomitantly, the shell forms around the cargo, pinching off excess cargo, which serves as a nucleus for biogenesis of the next carboxysome (55, 56). The formation of the shell around the procarboxysome is thought to start with the binding of CcmN, after which a C-terminal peptide of CcmN recruits the additional shell components CcmK2, CcmO, and CcmL, leading to the enclosure process (55). In the case of the α-carboxysome of *Halothiobacillus*, a cryo-electron tomography study suggested that the cargo and the shell assemble simultaneously (57). The α-carboxysome lacks the CcmM protein, which is thought to organize the β-procarboxysome, and the order of shell protein assembly has not been investigated. The assembly of MCPs other than the carboxysome has not yet been directly investigated. A process in which the shell pinches off excess cargo is reasonable, since mutants unable to form the shell of the Pdu MCP accumulate cargo proteins as enlarged polar bodies (22, 58). It is also of note that empty carboxysome and Pdu MCP shells can be produced by recombinant strains in the absence of cargo proteins (59, 60). In wild-type cells, simultaneous assembly of the shell and the cargo would help to minimize such events.

BMC Domain Proteins Are the Basic Building Blocks of the MCP Shell

The shells of bacterial MCPs are made primarily of a family of proteins whose structural core is the BMC domain, and variations upon this core provide functional diversity (11, 61–63). The first crystallographic structures of BMC domains were determined for the carboxysome shell proteins CcmK2 and CcmK4 (63). These proteins form flat hexamers, where one side is concave and the other is relatively flat. In some crystal forms, these hexamers tile edge-to-edge to form extended protein sheets. Thus, it was proposed that sheets of BMC domain proteins form the facets of the carboxysome shell (63). Later crystal structures showed that sheet formation was a conserved feature of many BMC domain proteins, and shell proteins were shown to form true two-dimensional (2D) layers *in vitro* by electron microscopy (64), thereby substantiating their role in shell formation. The initially characterized MCP shell proteins were about 100 amino acids in length and contained a single BMC domain. Later structures identified shell proteins whose monomers have two fused BMC domains. The double-BMC-domain proteins form trimers composed of six BMC domains in a pseudohexameric arrangement that is similar overall to that of the hexameric single-BMC-domain proteins (65–68). These trimers likely arose by gene duplication, and this variation may allow protein conformational changes by eliminating the strict 6-fold symmetry of the BMC domain hexamer (11). As described below, such structural rearrangements may allow BMC domain trimers to act as gated pores for metabolite transport across the MCP shell. Crystallographic studies have also found variants of hexameric and pseudohexameric BMC domain proteins where the BMC domain is circularly permuted (69). The tertiary structure of permuted BMC domain proteins is very close to that of the canonical BMC domain proteins, but the order of the structural elements is different. First observed for the PduU protein, domain permutations result in protein termini at different locations, allowing new functional elaborations at the ends of the polypeptide chain (69). Interestingly, for the structures determined so far, BMC domain proteins have a conserved flat hexagonal shape. Hence, it is thought that shape complementarity along the edges allows different types of shell proteins to tessellate into

mixed molecular sheets, with functional diversification arising from the variations of the individual BMC domain proteins.

Although a single-layer MCP shell is currently the favored model, some studies have suggested that the shell may be a double layer of BMC domain proteins (70, 71). A few crystal structures have found BMC domain proteins associated with their concave surfaces face-to-face, consistent with a double-layered shell (66, 70, 71). In addition, a recent solution study with the CcmK2 protein of *Thermosynechococcus* supports the idea of a double layer (71). However, it is difficult to explain how lumen enzymes would specifically associate with the inner face of a double-layered shell. In addition, an extended double-layer sheet has never been observed in crystals. Hence, the possibility of the MCP shell with a double layer or a partial double layer requires further study.

Pentamers Occupy the Vertices of the MCP Shell

Pentameric non-BMC-domain shell proteins are thought to form the vertices of MCPs and help impart the curvature needed to form a closed structure from the flat protein sheets of hexameric BMC domain proteins (62). Studies of large viruses have shown that pentagonal proteins at the vertices are used to form icosahedral capsids. Crystallography identified a class of pentameric MCP proteins that are encoded by most or all MCP operons (62). Genetic studies in several systems showed that a known pentamer or a pentamer homolog is required for MCP formation *in vivo* (48, 58, 72). In another study, the pentameric protein, CsoS4, of the α-carboxysome was not absolutely required for shell assembly but was required for shell closure and integrity (73). In another case, a conflicting result was initially obtained with regard to a pentamer homolog encoded by the *eut* operon. The EutN protein was found to be a hexamer in crystals (74). However, later studies showed that EutN was pentameric in solution, suggesting that the hexameric form may have been a minor species that selectively crystallized (75). Thus, pentameric vertex proteins are thought to be a widely conserved feature of MCP shells, and because of their key role in MCP formation, this class of proteins has been named bacterial microcompartment vertex (BMV) proteins (75).

The Central Pores of Some BMC Domain Proteins Are Thought To Act as Selectively Permeable Metabolite Conduits

Current models of MCP function require that the shell acts as a permeability barrier to a toxic or volatile intermediate while allowing the substrates, products, and cofactors of lumen enzymes to traverse the shell. This suggests that the shell is selectively permeable. The first crystal structures of BMC domain proteins revealed that they pack tightly together into extended two-dimensional layers with only a few small openings (63). The most notable openings were central pores that were proposed to function in selective metabolite transport (63, 68). Subsequent crystallography revealed that the pores of different BMC domain proteins diverge in their properties, consistent with a role in the selective transport of various metabolites (11, 12, 61). In the case of the carboxysome shell proteins CcmK1, CcmK2, and Ccmk4, the central pores are lined with positively charged residues that could reasonably promote the uptake of a negatively charged compound like bicarbonate, which is a primary substrate of the carboxysome (63). For the PduA protein, which is a component of an MCP used for 1,2-PD degradation, its central pore is lined with numerous H-bond donors and acceptors. This property is proposed to allow preferential movement of 1,2-PD compared to propionaldehyde, which must be held inside the MCP to prevent cellular toxicity (68). In addition, modeling suggests that the PduJ and PduK shell proteins have central pores similar to those of PduA and might also transport 1,2-PD. Thus, overall, MCP pores could control metabolite movement based on their steric/electrostatic properties, and within a single MCP, more than one shell protein could provide similar pores. We point out, however, that crystallographic studies have identified functionally diversified BMC domain proteins that lack small central pores, as described above. In some cases, the central pore is blocked; in other cases, it is replaced with a metal cluster (12, 14). Perhaps even more intriguing, some BMC domain proteins may have gated pores that are used to control metabolite movement across the MCP shell (66, 76).

The MCP Shell May Have Gated Pores

Recent studies have indicated that the MCP shells might contain gated pores that control the movement of metabolites between the MCP lumen and the cytoplasm of the cell. The first evidence of a gated pore was crystal structures that showed that a double-BMC-domain protein in the α-carboxysome (CsoS1D) can adopt two conformations: one where the central pore is open and another where it is closed (66, 76). This led to the proposal of a gated pore that opens and closes in response to a signal to allow metabolite movement across the MCP shell. Presumably, an incoming metabolite would bind the pore, which would open to allow passage and then close behind. This might allow relatively large compounds to cross the shell without compromising the ability of the MCP to minimize the escape of toxic/volatile metabolic intermediates. An alternative hypothesis is that gated pores in the MCP shell might work like an airlock. This idea is based on a recently reported crystal structure in which the CcmP protein formed a dimer of pseudohexamers with a central cavity formed where two concave surfaces come together (70). This would place a gated pore on either side of a central container in an airlock-like arrangement. It is also apparent that the open form of the gated pore is larger than the pores found in hexameric single-BMC-domain proteins, suggesting that it is used to allow the transport of bulkier metabolites. In the case of the carboxysome, larger pores could accommodate ribulose bisphosphate, the substrate of RuBisCO, or 3-phosphoglycerate, the product of the RuBisCO reaction. In addition, homologs of double-BMC-domain proteins having open and closed conformations have been found in operons for the Pdu and Eut MCPs as well as virtually all MCP operons (6, 67, 76, 77). In these cases, a large gated pore might mediate the movement of cofactors required by lumen enzymes, such as ATP, NAD/H, coenzyme A (HS-CoA), and coenzyme B_{12}. It is of note, however, that the *eut* and *pdu* operons each have only a single homolog with a predicted gated pore (EutL and PduB), and although not all of the shell proteins in these systems have been structurally characterized, the current body of structural data suggests that gated pores are only possible in these proteins. On the other hand, current models suggest that multiple enzymatic cofactors must pass through the shell, implying that either the shell proteins with gated pores allow the passage of distinct molecules or additional transport mechanisms may be involved, which are not yet understood. In addition, genomic studies have suggested that gated pores might be used to transport other classes of molecules, since CsoS1D and homologs (which are in the gated-pore

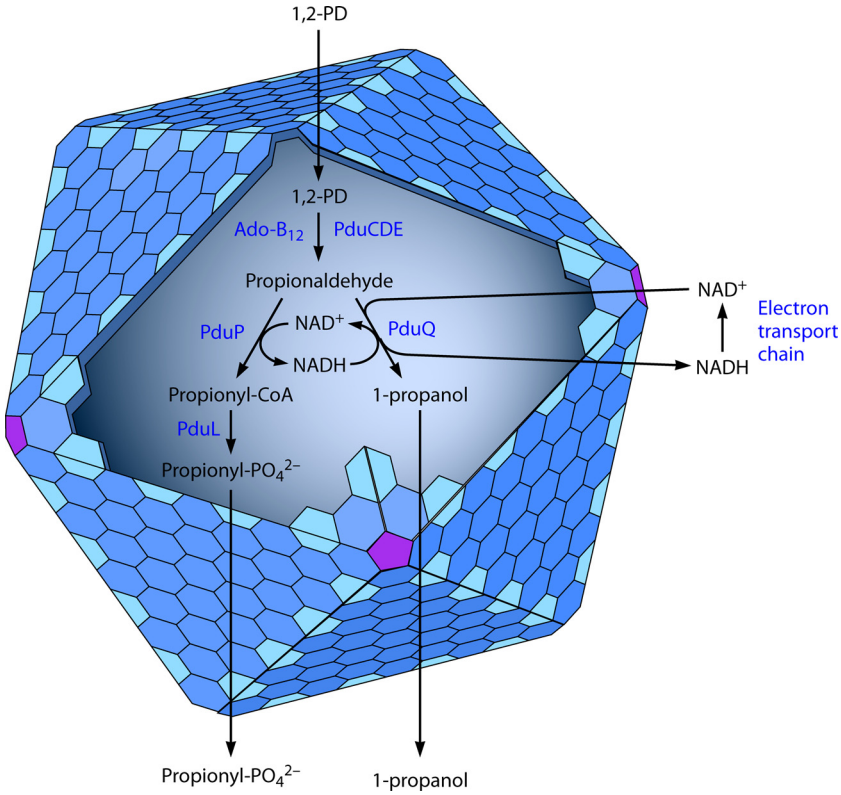

FIG 2 The enzymes encapsulated within MCPs are supplied with cofactors by internal and external recycling. Recent studies showed that the PduQ enzyme recycles NADH to NAD^+ internally within the Pdu MCP. NAD^+ is required for the activity of the PduP enzyme, which is essential for growth on 1,2-propanediol. However, because a PduQ mutant still grows at a rate about 50% of that of the wild type on 1,2-propanediol, external recycling is also indicated (79). In addition, studies of the Eut MCP have shown internal recycling of coenzyme A (81).

class of shell proteins) are often found proximal to enzymes and proteins of unknown function (11). A final observation is that the closing of the large central pores opens up three smaller pores that might promote the movement of enzyme substrates, suggesting a possible dual role of gated-pore-type shell proteins (65, 77). However, to date, no genetic or biochemical studies have directly substantiated the various structure-based models for molecular transport through BMC pores. Hence, the idea of selectively permeable pores as well as gated pores across the shell of MCPs requires further study.

Diverse BMC Domain Proteins May Function as Electron Conduits or Bind Nucleic Acids

Crystallographic studies have revealed a great deal of diversity in BMC domain proteins. The PduT protein has an iron-sulfur cluster where the central pore is typically found (60, 68, 78). It was proposed that PduT might act as an electron conduit between the cytoplasm of the cell and the MCP lumen. Alternatively, it might function as an iron-sulfur insertase that rebuilds damaged Fe-S centers of lumen enzymes or in redox regulation. However, as yet, no genetic or biochemical evidence supporting these hypotheses has been reported. Another MCP protein, EutK, has a BMC domain fused to a helix-turn-helix DNA/RNA binding domain. Presumably, EutK might have a role in regulating the expression of BMC domain proteins, but potential regulatory signals are not clear at this time. In addition, a number of BMC domains are found fused to domains of unknown function, some of which are apparently disordered and might participate in protein-protein binding interactions (11, 12). Thus, overall, a great deal still remains to be learned about the functional diversity of BMC domain proteins.

Enzymatic Cofactors Are Internally Recycled within MCPs, at Least in Part

The first studies to show that cofactors are recycled internally within bacterial MCPs were recently reported by Cheng et al., who showed that the primary role of the PduQ enzyme is to recycle NAD/H within the lumen of the Pdu MCP (79). However, these studies indicated that a portion of NAD/H recycling was also mediated by the electron transport chain, which would require cofactor transport across the MCP shell (Fig. 2) (79). In the Pdu MCP, the role of the PduQ 1-propanol dehydrogenase is to regenerate NAD^+ from NADH during fermentative growth. However, Cheng et al. found that a *pduQ* deletion mutant of *Salmonella* grew at a reduced rate on 1,2-PD under aerobic conditions (79). This was somewhat unexpected since the electron transport chain is available to regenerate NAD^+ during aerobic growth. A possible explanation is that the PduQ enzyme is needed to provide extra capacity for NAD^+ regeneration beyond that available through the electron transport chain or that the role of the PduQ enzyme is to recycle NAD^+ internally within the Pdu MCP. Further studies showed that ectopic expression of a non-MCP-associated alcohol dehydrogenase could not correct the *pduQ* growth defect even when its total enzymatic activity exceeded that of the PduQ en-

zyme. This finding was contrary to the idea that the role of the PduQ enzyme was to provide extra NAD/H recycling capacity. Further studies showed that genetic disruption of the Pdu MCP eliminated the slow-growth phenotype of the *pduQ* deletion mutant, indicating that PduQ has an MCP-specific function. The latter finding was supported by *in vitro* studies with purified MCPs which showed that the PduQ enzyme could regenerate NAD^+ to support the activity of the PduP propionaldehyde dehydrogenase (PDH). Thus, *in vitro* and *in vivo* evidence indicates that the primary role of the PduQ enzyme is to support the activity of the PduP aldehyde dehydrogenase by recycling NADH to NAD^+ internally within the Pdu MCP. However, the studies by Cheng et al. also showed that the *pduQ* deletion mutant was still able to grow on 1,2-PD at a reduced rate. This would be possible only if NAD^+ can be regenerated independently of the PduQ enzyme. It was proposed that some NADH exits the MCP via specific pores, is oxidized back to NAD^+ by the electron transport chain, and then reenters the MCP. Thus, supplying the enzymes of the Pdu MCP with NAD^+/NADH is thought to require both internal recycling and transport across the protein shell via specific pores. Studies with the Pdu system also showed that all of the enzymes needed for adenosylcobalamin (Ado-B_{12}) recycling were components of purified MCPs, and it was therefore proposed that cobalamin recycling can also occur internally within the Pdu MCP (80).

Recent studies of the Eut MCP indicated internal recycling of coenzyme A (81). For the Eut MCP, the EutD enzyme recycles HS-CoA, and growth on ethanolamine is essentially abolished by a *eutD* deletion mutant. Consequently, it was proposed that CoA is unable to cross the shell of the Eut MCP and must be internally recycled. Extrapolation of this finding led to the proposal that no large cofactors cross the shell of the Eut MCP. It was suggested that NAD/H and CoA are internally recycled, that the EutBC ethanolamine ammonia lyase (EAL) and its reactivation factor (which require B_{12} and ATP) are associated with the outer surface of the MCP shell (rather than being encapsulated), and that the acetaldehyde produced by EutBC is injected into the lumen of the Eut MCP. In this model, specific pores are not needed for cofactor transport. In its current form, this model does not apply to the Pdu MCP, where the enzyme that converts 1,2-PD to propionaldehyde (diol dehydratase) has been localized to the interior of the Pdu MCP (22). Further work will be needed to understand the biochemical details of the Eut MCP.

1,2-PROPANEDIOL DEGRADATION AND THE Pdu MCP

For many years, the carboxysome was the only known MCP, and it seemed to be unique, a specialized organelle used to enhance the catalytic activity and specificity of RuBisCO, a slow, relatively nonspecific enzyme. Then, in 1994, genetic studies and sequence analyses showed that the PduA protein (which is encoded by an operon involved in B_{12}-dependent 1,2-PD degradation by *Salmonella*) had relatively high sequence identity to the carboxysome shell protein CcmK (4). Consequently, it was proposed that a carboxysome-like structure might be involved in 1,2-PD degradation (4). A few years later, Bobik and coworkers showed that *Salmonella* conditionally forms polyhedral bodies similar in size and shape to carboxysomes during growth in the presence of 1,2-PD but not during growth on a variety of other carbon sources (6, 22). The Pdu MCPs are polyhedral and about 100 to 150 nm in diameter. They consist of a protein shell that encapsulates enzymes and cofactors used for 1,2-PD degradation. The mass of a Pdu MCP is about 600 MDa, and it is estimated to include 18,000 individual polypeptides of 18 to 20 different types (17). It is thought that the Pdu MCPs are made completely of protein subunits, and there is no evidence that they contain nucleic acid, carbohydrate, or lipid components. The shells of the Pdu MCP are built primarily from BMC domain proteins and also include a BMV pentamer that forms the vertices (6). A variety of studies indicate that the Pdu MCPs are used to optimize growth on 1,2-PD by sequestering a toxic/volatile pathway intermediate (propionaldehyde) (6, 22, 58, 79, 80, 82–84).

Ecology of 1,2-PD Degradation

1,2-PD is a major product of the fermentation of two common plant sugars, rhamnose and fucose (85, 86). These sugars are common in plant cell walls, bacterial capsules, and the glycoconjugates of eukaryotic cells. Hence, 1,2-PD metabolism is thought to be especially important in anaerobic environments such as the large intestines of higher animals, sediments, and the depths of soils. Genes for B_{12}-dependent 1,2-PD degradation are found in a number of soil-dwelling and enteric bacteria, including *Salmonella*, *Klebsiella*, *Shigella*, *Yersinia*, *Listeria*, *Lactobacillus*, *Lactococcus*, *Clostridium*, and at least one strain of *Escherichia coli* (E24377A) (9, 15, 17). In all cases examined, *pdu* gene clusters are highly conserved, indicating that MCPs are essential for 1,2-PD degradation (17). Analyses of *pdu* gene clusters also suggest frequent horizontal gene transfer and operon reorganization as well as conditional selective pressure (6, 20, 29). In addition, a number of studies have indicated that 1,2-PD degradation plays a role in enteric pathogenesis and is important for growth in the intestinal environment, as described above (30, 34).

Pathway of 1,2-PD Degradation

The pathway of 1,2-PD degradation begins with the conversion of 1,2-PD to propionaldehyde by coenzyme B_{12}-dependent diol dehydratase (28, 85–87) (Fig. 3). Propionaldehyde is oxidized to propionyl-CoA by propionaldehyde dehydrogenase, or alternatively, it is reduced to form 1-propanol by 1-propanol dehydrogenase (6, 85–87). Under fermentative conditions, propionyl-CoA is converted by a phosphotransacylase (PTAC) to propionyl-phosphate and then by a reversible propionate kinase to propionate, producing one molecule of ATP by substrate-level phosphorylation (88). However, 1,2-PD fermentation does not produce a source of carbon for biosynthetic reactions, since 1-propanol is excreted in order to eliminate excess reducing equivalents (38). Thus, *Salmonella* does not grow on 1,2-PD as a sole carbon and energy source under fermentative conditions. 1,2-PD metabolism does, however, enhance cell yield by providing additional ATP when a small amount of yeast extract is added to growth medium to provide biosynthetic building blocks (89).

Under aerobic conditions, *Salmonella enterica* is able to grow on 1,2-PD as a sole carbon and energy source (87). In this case, some propionyl-CoA is converted to propionate, but a portion also feeds into the methyl citrate pathway (90, 91). The methyl citrate pathway is an aerobic pathway used for metabolism of propionate/propionyl-CoA derived from diverse carbon sources. It does not function under anaerobic conditions. The genes for the methyl citrate pathway are found outside the *pdu* operon at the *prp* locus (90, 91). In this pathway, propionyl-CoA is joined to oxaloacetate to form methyl citrate, which is subsequently converted to succinate and pyruvate. Pyruvate is metabolized further

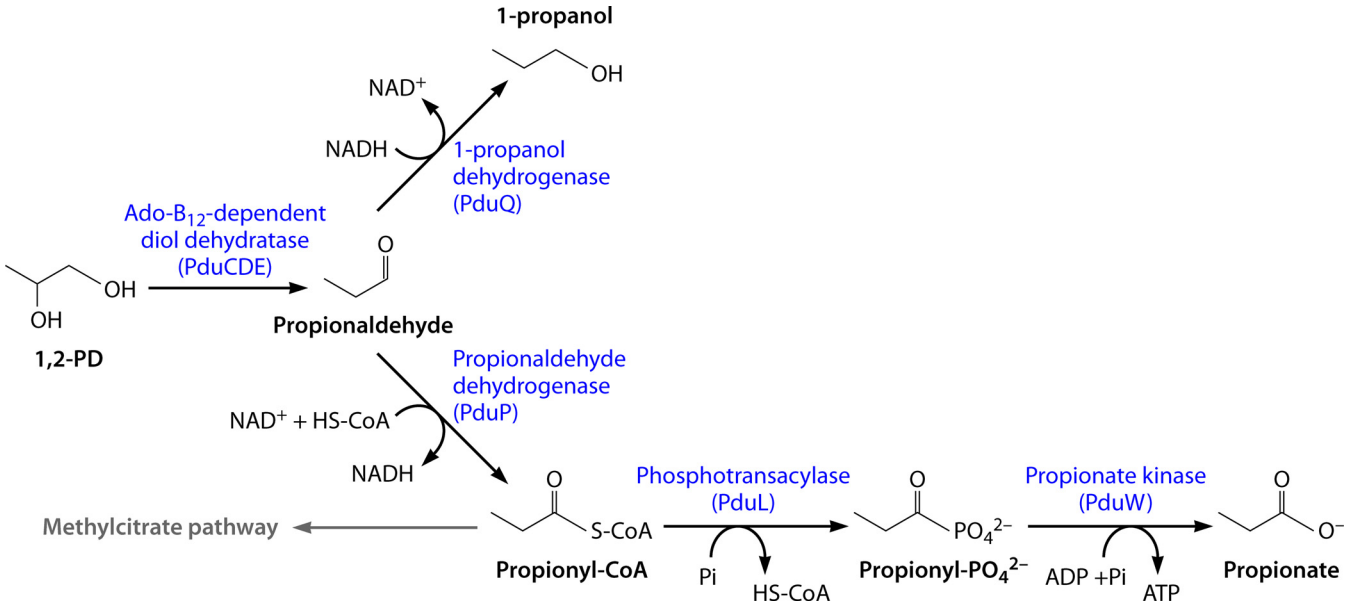

FIG 3 Pathway of 1,2-propanediol degradation. Under fermentative conditions, the pathway of 1,2-propanediol degradation provides a source of ATP and reducing power (NADH) but no source of cell carbon. Under aerobic conditions or during anaerobic respiration with tetrathionate, propionyl-CoA feeds into the methyl citrate pathway to provide additional ATP as well as biosynthetic building blocks.

to acetyl-CoA, which enters the tricarboxylic acid (TCA) cycle. *Salmonella* strains carrying *prp* mutations are unable to grow on 1,2-PD as a sole carbon and energy source (92).

Salmonella can also use 1,2-PD also as a sole carbon and energy source during anaerobic respiration with tetrathionate as the terminal electron acceptor (38). Interestingly, tetrathionate (a somewhat obscure chemical) is found in the inflamed gut, where it provides a substantial growth advantage to *Salmonella*, as described above (33). More common terminal electron acceptors for anaerobic respiration, such as nitrate, fumarate, dimethyl sulfoxide (DMSO), and trimethylamine N-oxide (TMAO), have not been shown to support the anaerobic respiration of 1,2-PD, and the reason why they are unable to do so is currently unclear.

Growth on 1,2-PD Requires Coenzyme B_{12}

Growth of *Salmonella* on 1,2-PD requires coenzyme B_{12} (adenosylcobalamin [Ado-B_{12}]), which is an essential cofactor for diol dehydratase, the first enzyme in the pathway (87). *Salmonella* synthesizes B_{12} *de novo* only under strict anaerobic conditions (93). Consequently, growth of *Salmonella* on 1,2-PD in the presence of oxygen requires supplementation of the growth medium with complex precursors such as vitamin B_{12} (cyanocobalamin [CN-B_{12}]), which *Salmonella* can convert to Ado-B_{12} even when O_2 is present. The paradox that *Salmonella* synthesizes B_{12} *de novo* only under anaerobic conditions but cannot grow by the fermentation of 1,2-PD was previously pointed out (88). Subsequently, however, it was shown that the respiration of 1,2-PD with tetrathionate supported growth with the *de novo* synthesis of B_{12} (38). This apparently resolved the paradox that *Salmonella* synthesizes B_{12} *de novo* only in the absence of oxygen but is unable to grow on 1,2-PD (and ethanolamine) by fermentation (38).

Genes for 1,2-PD Degradation

The genes required for 1,2-PD degradation form a contiguous cluster at the *pdu* locus on centisome 44 of the *S. enterica* chromosome (4, 6, 87). This locus appears to include all the structural proteins and enzymes that comprise the Pdu MCP as well as the regulatory genes that control its production (6, 82). The *pocR* and *pduF* genes are adjacent to and divergently transcribed from the main *pdu* operon (Fig. 4) (4, 94). The *pocR* and *pduF* genes encode a positive transcriptional regulatory protein and a 1,2-PD diffusion facilitator, respectively (4, 95, 96). The *pdu* operon includes 22 *pdu* genes, *pduABB′CDEGHJKLMNOPQSTUVWX*, that encode 1,2-PD degradative enzymes (PduCDELPQW), B_{12} recycling proteins (PduGHOSX), as well as BMC domain proteins and other MCP-related proteins (PduMV) (4, 6).

Regulation of the Genes for 1,2-PD Degradation

The genes for 1,2-PD degradation are contiguous and coregulated with 20 genes (of about 30 total) used for the *de novo* synthesis of cobalamin (*cob*) (Ado-B_{12}) (95–97). Both the *cob* and *pdu* genes are induced in response to 1,2-PD during growth on poor carbon sources (87, 95, 96). This scheme makes sense, as it allows the coproduction of the 1,2-PD degradative pathway together with its required cofactor. Furthermore, coregulation suggests that 1,2-PD catabolism is a primary reason for *de novo* B_{12} synthesis in *S. enterica* (88). If one counts both the *cob* and *pdu* genes, *Salmonella* devotes over 1% of its genome to 1,2-PD degradation, suggesting that these genes are under strong selection in natural environments (88).

Both local and global systems coregulate the *cob* and *pdu* genes (95, 96, 98). Local control requires the PocR transcription factor, which activates transcription when bound by its coeffector 1,2-PD (99). Global control is mediated by the cyclic AMP receptor protein-cyclic AMP complex (CRP-cAMP) and the two-component ArcA/ArcB system, which sense carbon availability and environmental redox potential, respectively (94, 98, 100, 101). Induction occurs both aerobically and anaerobically when 1,2-PD is present and cAMP-CRP levels are sufficiently high. Induction does not

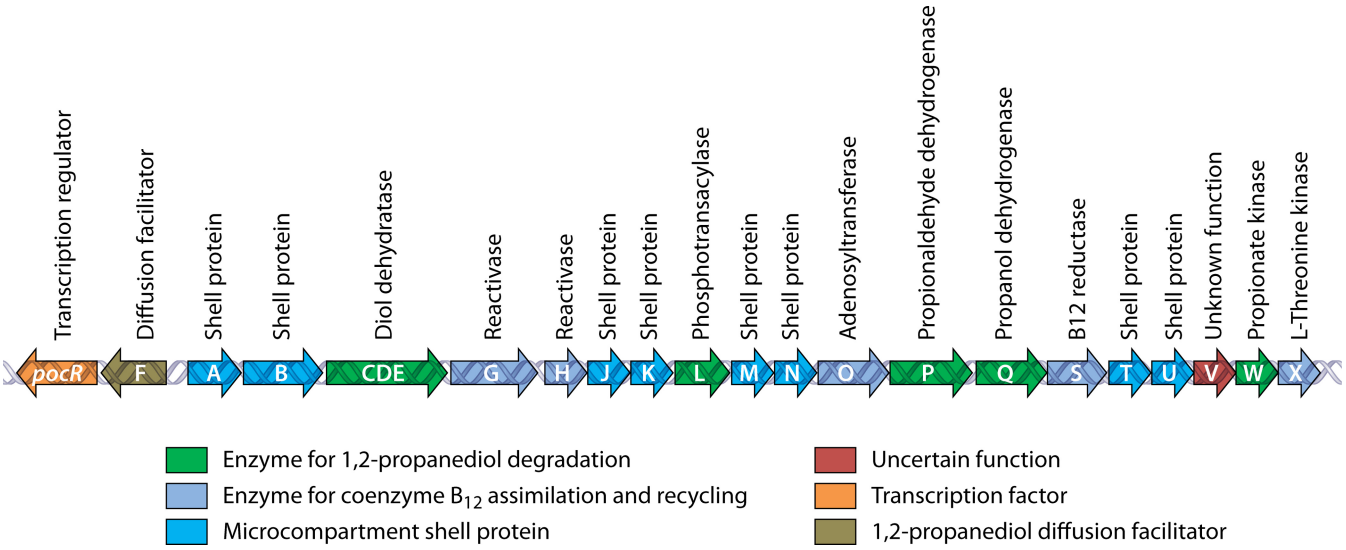

FIG 4 The *pdu* locus of *Salmonella enterica*. The genes involved in 1,2-PD degradation, including those for MCP formation, cluster at a single locus. The genes for MCP formation are interspersed with those encoding pathway enzymes. This general arrangement is found for many MCP operons, although in some cases, the genes may be dispersed.

require the ArcA/ArcB system, but under anaerobic conditions, ArcA/ArcB and CRP-cAMP have an additive effect that increases the maximal expression level. Overall, the *cob* and *pdu* operons are induced by 1,2-PD both aerobically and anaerobically in the absence of preferred carbon sources such as glucose.

The Pdu MCP Functions To Minimize Propionaldehyde Toxicity

The proposed function of the Pdu MCP is to sequester propionaldehyde to prevent cytotoxicity, DNA damage, and carbon loss to the environment; propionaldehyde is poorly retained by the bacterial cell envelope (22, 24). The initial clue for this idea is based on the observation that both 1,2-PD and ethanolamine degradation genes are found in operons that contain homologs of carboxysome shell proteins (4, 5). Both of these processes proceed by analogous pathways with aldehyde intermediates (propionaldehyde and acetaldehyde, respectively). Hence, it was suggested that MCPs might sequester toxic aldehydes formed during 1,2-PD and ethanolamine degradation (5). Later studies showed that shell mutants unable to form the Pdu MCP accumulate propionaldehyde to toxic levels during growth on 1,2-PD (22, 24). These mutants undergo a 20-h period of growth arrest due to propionaldehyde toxicity and are subject to increased mutation rates during growth on 1,2-PD. The explanation for why *Salmonella* overcomes propionaldehyde toxicity and resumes growth after about 20 h is that 1,2-PD metabolism continues during this period even though cells are not growing (22, 24). Over time, 1,2-PD is completely consumed, halting the formation of propionaldehyde. Subsequently, propionaldehyde is depleted by conversion to propionate and 1-propanol, at which time growth of *Salmonella* resumes, with propionate and 1-propanol serving as the carbon and energy sources (22, 24). The aldehyde toxicity model is further supported by the findings that *polA* (DNA repair polymerase) and *gsh* (glutathione biosynthesis) mutants are unable to grow on 1,2-PD or ethanolamine (23, 102). Thus, several lines of evidence support the idea that the Pdu MCP functions to mitigate propionaldehyde toxicity (Fig. 5).

Besides propionaldehyde toxicity, an additional phenotype of mutants unable to form the Pdu MCP is that they grow faster than the wild type at limiting levels of B_{12} (22). This phenotype is seen for a variety of shell mutants, providing solid support for the idea that faster growth results from a shell defect (58, 103). At limiting B_{12} levels, propionaldehyde toxicity is not observed due to decreased activity of B_{12}-dependent diol dehydratase, the enzyme that produces propionaldehyde from 1,2-PD. The current explanation for why MCP mutants grow faster than the wild type at limiting B_{12} levels is that the shell acts as a barrier that regulates/impedes the movement of substrates and cofactors into and out of the MCP. In the absence of the shell, enzymatic activities increase due to improved substrate availability. However, when the B_{12} supply is sufficient, a shell defect leads to propionaldehyde accumulation, which results in toxicity and DNA damage, as described above.

Purification, Composition, and Enzymology of the Pdu MCP

The Pdu MCP from *S. enterica* serovar Typhimurium LT2 was purified intact (Fig. 6) (82). 2D electrophoresis followed by proteomics analyses identified 14 different polypeptide components (PduABB′CDEGHJKOPTU). Subsequent studies determined that 4 additional proteins (PduMNQS) are tightly associated with the Pdu MCP and that the PduV protein might be associated with the outer surface of the shell (48, 58, 79, 80, 84). Of the 19 polypeptides that are components of the Pdu MCP, 8 (PduABB′JKNTU) are likely shell components, PduM and PduV are of uncertain function, and 9 polypeptides are subunits of six enzymes: B_{12}-dependent diol dehydratase (DDH) (PduCDE), DDH reactivase (PduGH), propionaldehyde dehydrogenase (PduP), 1-propanol dehydrogenase (PduQ), cobalamin reductase (PduS), and adenosyltransferase (ATR) (PduO) (6, 28, 79, 80, 83, 89, 104–107). DDH, propionaldehyde dehydrogenase, and 1-propanol dehy-

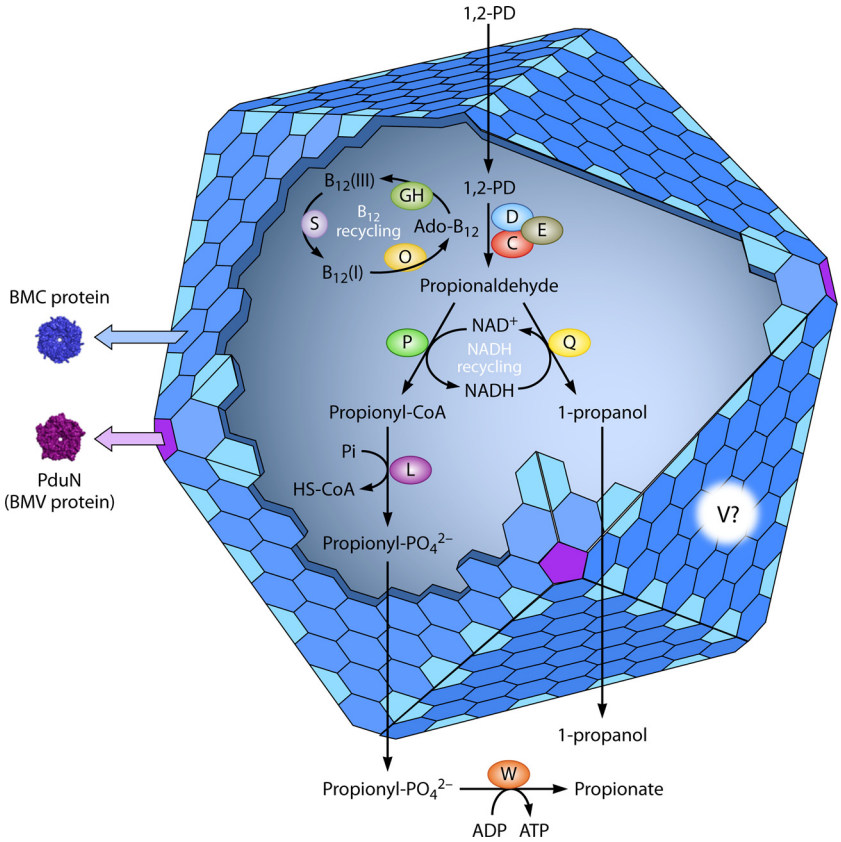

FIG 5 Model for 1,2-propanediol degradation by *S. enterica*. 1,2-PD degradation occurs within the Pdu MCP. The function of the MCP is to sequester propionaldehyde to prevent toxicity and carbon loss. The first step of 1,2-PD degradation is its conversion to propionaldehyde. The protein shell of the Pdu MCP acts as a diffusion barrier and helps to channel propionaldehyde to propionaldehyde dehydrogenase and 1-propanol dehydrogenase. It is thought that propionyl-phosphate leaves the MCP and feeds into the methyl citrate pathway, which provides additional energy and biosynthetic building blocks.

drogenase are highly active in purified MCPs (82, 83). The activities of the other associated enzymes have not been measured by using purified MCPs. The presence of highly active enzymes indicates that the Pdu MCP is a metabolically active organelle. Results have also shown that measurement of PduCDE, PduP, and PduQ activities requires the addition of appropriate substrates and cofactors to enzymatic assay mixtures, showing that the Pdu MCPs as purified are permeable to the metabolites and cofactors of 1,2-PD degradation (79, 82, 83). The detailed mechanisms by which substrates, products, and cofactors enter and exit the Pdu MCP have not been worked out fully, but specific pores centrally located in BMC domain shell proteins provide the most plausible routes for transit, as described above.

Enzymes of the 1,2-PD Degradative Pathway

The B_{12}-dependent PduCDE diol dehydratase. In the first step of 1,2-PD degradation, coenzyme B_{12}-dependent DDH catalyzes the conversion of 1,2-PD to propionaldehyde (28, 108). DDH has three nonidentical subunits, encoded by the *pduCDE* genes, in a stoichiometry of $\alpha_2\beta_2\gamma_2$ (28). The PduCDE DDH is the major enzymatic component of the Pdu MCP, comprising about one-third of its total mass (82). Mutations that inactivate the PduCDE enzyme prevent growth on 1,2-PD, showing that it is essential for this process (28, 109). DDH enzymes are closely related in sequence to B_{12}-dependent glycerol dehydratase (GDH) used by many genera of bacteria for glycerol fermentation (43, 85). DDH enzymes have been purified and characterized from several sources (110–114). No structure is currently available for the PduCDE enzyme from *Salmonella enterica*. However, the crystal structure of a homologous protein, PddABC from *Klebsiella oxytoca*, has been reported (115). The PduCDE subunits of *Salmonella* share 94, 92, and 93% identities with the α, β, and γ subunits, respectively, of the PddABC enzymes in *Klebsiella*. The structure of the *Klebsiella* enzyme reveals its composition as a dimer of heterotrimers, $(\alpha\beta\gamma)_2$ (115). The three subunits interact to maintain the overall structure. By sequence analysis, it was observed that 20 and 16 amino acids at the N termini of the β and γ subunits, respectively, are missing from GDH enzymes (43, 44). Studies with the *Klebsiella* enzyme showed that these extensions were not essential for enzymatic activity but did substantially affect the solubility of the protein, with truncated proteins becoming much more soluble (44). More recent studies, described above, determined that the N-terminal sequence of the β subunit (PduD) of DDH from *Salmonella* targets itself and the PduCDE subunits into the Pdu MCP (39). However, no evidence that the N-terminal extension on the γ subunit has a role in MCP localization could be obtained.

The PduL phosphotransacylase. The PduL phosphotransacylase (PTAC) catalyzes the interconversion of propionyl-PO_4^{2-} and propionyl-CoA. Liu et al. reported biochemical and genetic studies establishing that PduL is a new class of PTAC and demon-

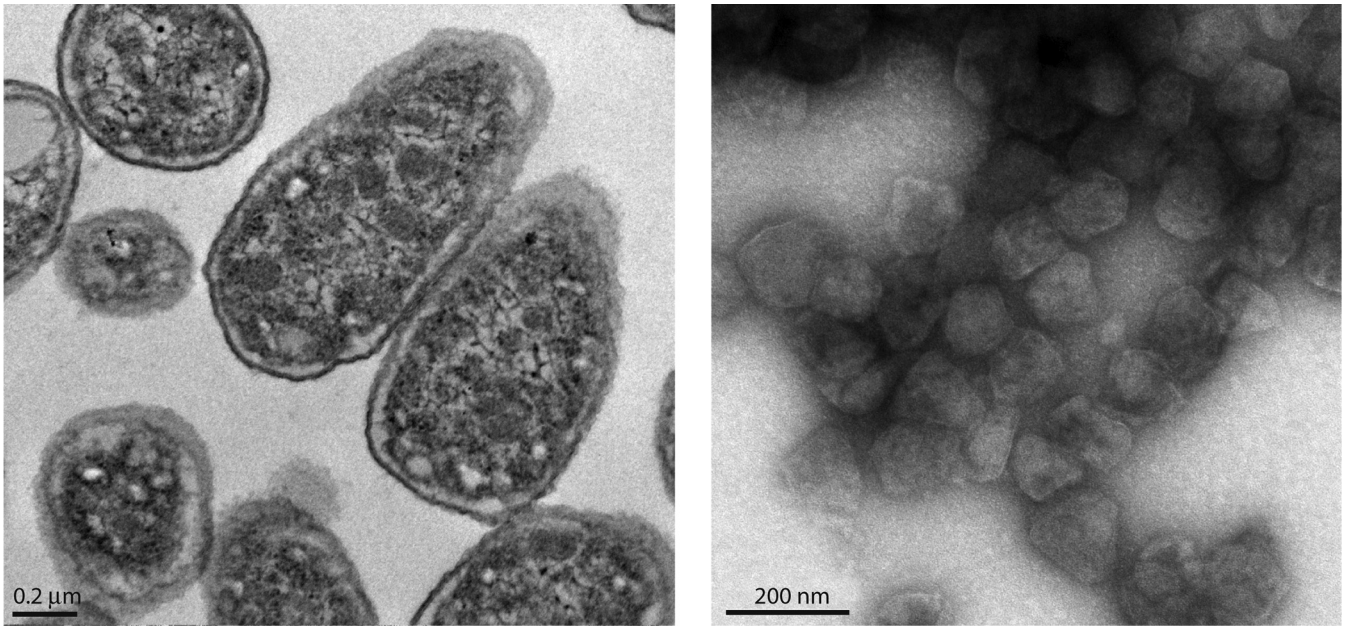

FIG 6 Electron micrographs of Pdu microcompartments from *S. enterica*. (Left) Thin sections of whole cells. (Right) Purified microcompartments.

strating its role in 1,2-PD degradation (89). The PduL enzyme has relatively high PTAC activity and reasonably low K_m values (89). Genetic analyses have shown that *pduL* mutants are unable to ferment 1,2-PD and grow slowly under aerobic conditions, demonstrating the role of PduL in 1,2-PD catabolism (89). BLAST and PSI-BLAST analyses have shown that PduL lacks significant similarity to known PTAC enzymes (89). PduL consists of 210 amino acids, while other PTAC representatives in *Salmonella enterica*, Pta and EutD, are 714 and 338 amino acids, respectively. Recent studies have shown that a PTAC enzyme encoded by the *eut* operon (EutD) is used to recycle CoA internally within the Eut MCP (81). PduL could have a similar role in the Pdu MCP (81).

The PduP propionaldehyde dehydrogenase. The PduP propionaldehyde dehydrogenase (PDH) catalyzes the conversion of propionaldehyde plus HS-CoA and NAD^+ to propionyl-CoA plus NADH (83). Null mutations in the *pduP* gene prevent growth on 1,2-PD, establishing its essential role in this process (83). The PduP enzyme of *Salmonella* has been purified with an N-terminal His tag and partially characterized (83). An enzyme assay showed that it has high levels of PDH activity, and mass spectrometry established propionyl-CoA as a reaction product. The PduP enzyme of *Salmonella* was also shown to be an MCP component by immuno-EM and by analysis of purified MCPs, which were found to be about 8% PduP (82, 83). Recent studies showed that a short N-terminal sequence targets PduP to the interior of the MCP, as described above (40). Homologs of PduP from other organisms have been purified and studied biochemically (116, 117). Some PduP homologs show broad enzymatic activity on various aliphatic aldehydes, including 3-hydroxypropionaldehyde (HPA), as evident from studies with the *Klebsiella pneumoniae* and *Lactobacillus reuteri* enzymes (116, 117). These homologs, which share ~86% amino acid sequence identity with the *Salmonella* PduP enzyme, are used for production of 3-hydroxypropionic acid during glycerol degradation (116, 117).

The PduQ 1-propanol dehydrogenase. Cheng et al. demonstrated in 2012 that PduQ is a part of the Pdu MCP and that it has 1-propanol dehydrogenase activity (79). Results also showed that this enzyme is oxygen sensitive and helps recycle NAD^+ internally within the Pdu microcompartment in order to supply the oxidized cofactor required for propionaldehyde dehydrogenase (PduP). However, studies indicated that NAD^+ regeneration also occurs via the electron transport chain, which requires movement of NAD^+/NADH across the MCP shell (79), as more fully described above.

The PduW enzyme is a propionate kinase. The PduW enzyme is a propionate kinase that catalyzes the conversion of propionyl-phosphate to propionate in a reaction that is coupled to the production of ATP from ADP plus inorganic phosphate (92). This reaction provides a source of ATP during the fermentation of 1,2-PD by *Salmonella* (86, 92). However, PduW also works in the reverse direction to allow the reuptake of propionate derived from 1,2-PD (92). During growth on 1,2-PD, a significant percentage of the initial carbon available to the cell as 1,2-PD is excreted into the medium as propionate (90, 92). Subsequently, PduW works in concert with the housekeeping phosphotransacetylase (Pta) as well as acetyl-CoA and propionyl-CoA synthases (Acs and PrpE, respectively) to recapture exogenous propionate via conversion to propionyl-CoA, which feeds into the methyl citrate pathway, supporting growth (91, 118). The use of PduW and Pta is preferred at high propionate concentrations, whereas Acs and PrpE are required for efficient growth when propionate levels are low (92).

Enzymes for Reactivation of Diol Dehydratase and B_{12} Recycling

The first enzyme in 1,2-PD degradation, B_{12}-dependent DDH, is subject to mechanism-based inactivation (119, 120). Consequently, 1,2-PD degradation requires systems for DDH reactivation and B_{12} recycling (121). During DDH catalysis, the adenosyl group of Ado-B_{12} is periodically lost due to catalytic by-reactions and replaced with an alternative upper ligand, usually a hydroxyl

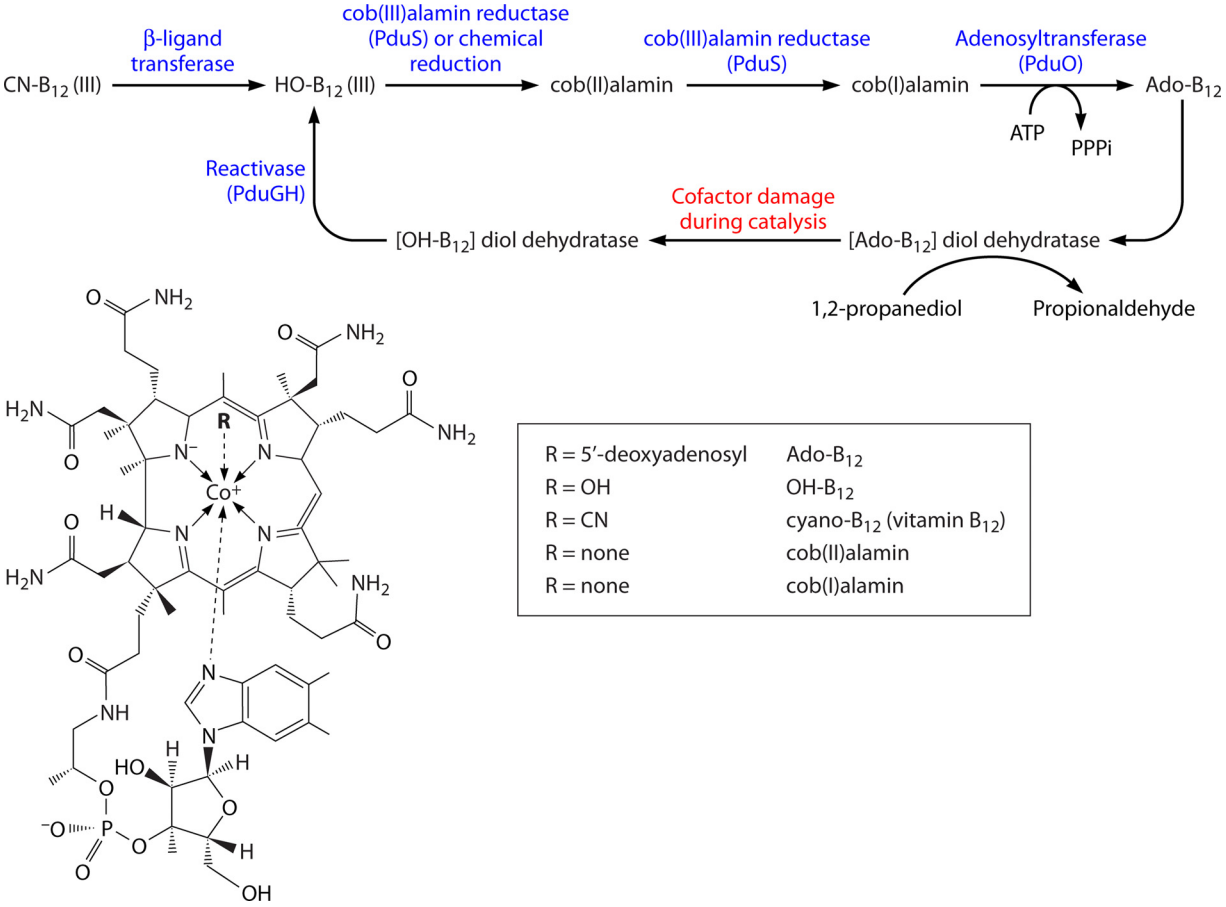

FIG 7 Vitamin B_{12} assimilation and recycling. The first step of 1,2-propanediol degradation is catalyzed by coenzyme B_{12}-dependent diol dehydratase. To supply diol dehydratase with its required cofactor, vitamin B_{12} (CN-B_{12}) can be taken up from the environment and converted to the active coenzyme Ado-B_{12}. During substrate turnover, catalytic by-reactions sometimes convert Ado-B_{12} to HO-B_{12}, which remains enzyme bound. HO-B_{12} is removed from diol dehydratase by the PduGH reactivase and then converted back to Ado-B_{12} by a pathway similar to that used for assimilation of coenzyme B_{12} from the environment.

group, resulting in the formation of an inactive [OH-B_{12}-DDH] complex (120, 122). Reactivation begins with the PduGH reactivase, which converts the inactive [OH-B_{12}-DDH] to free OH-B_{12} and apoenzyme (120, 122–127). Subsequently, Ado-B_{12} spontaneously reassociates with apo-DDH to form an active holoenzyme, and the OH-B_{12} is recycled back to Ado-B_{12} by cobalamin reductase (PduS) and adenosyltransferase (PduO) (80, 104, 105) (Fig. 7). The PduGH, PduS, and PduO enzymes are encoded by the *pdu* operon, and all these enzymes are associated with the Pdu MCP, suggesting that DDH reactivation and OH-B_{12} recycling occur within the MCP lumen (80, 104, 105). The PduS and PduO enzymes are also used for the assimilation of exogenous OH-B_{12} and are redundant with a set of constitutively expressed enzymes for this process (128–130).

The PduS B_{12} reductase. Sampson et al. first reported that the PduS enzyme of *Salmonella* is a B_{12} reductase that catalyzes the reduction of OH-B_{12} to cob(I)alamin in two one-electron steps (80, 106, 107) (Fig. 7). PduS is part of a B_{12} recycling pathway used to supply Ado-B_{12} to DDH (see above), and recent studies have shown that PduS is a component of the Pdu MCP (80). Strains with *pduS* mutations are only marginally impaired in 1,2-PD degradation due to the fact that *Salmonella* has redundant systems for B_{12} reduction (80, 128–130). Although PduS has both cob(III)alamin and cob(II)alamin reductase activities *in vitro*, it is thought that only the cob(II)alamin reductase activity is relevant *in vivo*, since cob(III)alamin reduction occurs as a spontaneous reaction under reducing conditions in the cytoplasm. On the other hand, however, it cannot be ruled out that the environment inside the Pdu MCP is more oxidizing than the general cytoplasm, as has been suggested for carboxysomes (56, 131).

The PduS enzyme of *Salmonella* is 451 amino acids in length. It contains two canonical 4Fe-4S motifs (^{264}CX2CX2CX3C^{274} and ^{309}CX2CX2CX4C^{320}) and a nonclassical Rossmann fold proposed to bind flavin mononucleotide (FMN) (^{120}YX2G[D/E]E^{125}) (80). It also has an NADH binding motif (^{28}GXGXG^{33}) and an N-terminal glycine-rich loop (^{25}GX2GXGGAG[F/L]P[A/T]X2K^{39}) proposed to bind the ADP moiety of NADH. Lastly, PduS has a soluble ligand binding β-grasp (SLBB) fold proposed to bind B_{12}, and this is supported by *in vitro* binding studies (106). Biochemical studies have also shown that PduS is an oxygen-sensitive iron-sulfur flavoprotein and that each monomer contains one molecule of noncovalently bound FMN as well as two coupled 4Fe-4S centers (80, 106). The reduction of cob(II)alamin to cob(I)alamin by PduS is measured by a linked assay with an adenosyltransferase [which converts cob(I)alamin to Ado-B_{12}] or by trapping cob(I)alamin with iodoacetate (107). Direct measurement of cob(I)alamin is difficult due to its high reactivity. *In vitro* studies indicate

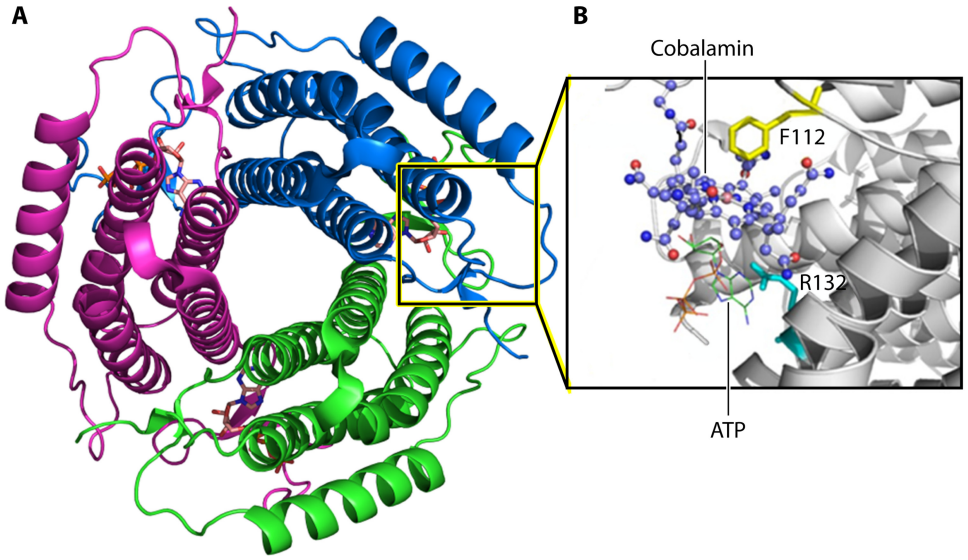

FIG 8 Structure of the PduO adenosyltransferase of *Lactobacillus reuteri*. The structure shown corresponds to the N-terminal ATR domain of PduO from *Salmonella*. (A) PduO in complex with cobalamin and ATP. (B) Residues interacting with ATP and cobalamin are labeled.

that the substrate of PduS is cob(II)alamin bound to an ATR. When cob(II)alamin binds ATR, it undergoes a transition to the 4-coordinate base-off conformer (132–135). Transition to this state raises the midpoint potential of the cob(II)alamin/cob(I)alamin couple by about 250 mV, facilitating reduction.

The PduO adenosyltransferase. Johnson et al. determined that the PduO enzyme of *Salmonella* is an ATR that catalyzes the terminal step of B_{12} assimilation, the conversion of cob(I)alamin and ATP to the coenzyme Ado-B_{12} and triphosphate (105). PduO was the founding member of a new class of ATR enzymes. PduO-type ATRs are the most widespread in nature and are found in higher animals (105, 136–138). As mentioned above, PduO is a component of the Pdu MCP and is thought to be required for recycling B_{12} within this organelle (82). Strains with a *pduO* deletion mutation are only slightly impaired for growth on 1,2-PD due to functional redundancy with the CobA adenosyltransferase (105). Double mutants lacking both *pduO* and *cobA* are unable to synthesize Ado-Cbl and do not grow on 1,2-PD (105, 128). As expected, growth of these double mutants on 1,2-PD is partially corrected by supplementation of media with Ado-B_{12} (105).

Sequence analyses show that the PduO enzyme of *Salmonella* consists of two domains (104). The N-terminal domain, which is about 185 amino acids in length, catalyzes the adenosyltransferase reaction (104). The C-terminal domain (about 150 amino acids in length) is a widely conserved domain of unknown function (DUF336). Although the three-dimensional structure of PduO of *Salmonella* has not been characterized, crystal structures for the PduO N-terminal ATR domains from *Lactobacillus reuteri* and several other organism have been reported (133, 139, 140). For *Lactobacillus*, cocrystallization of the PduO protein with ATP and cob(II)alamin reveals the molecular features of four-coordinate cob(II)alamin stabilization at its active site, where the corrin ring is found in a hydrophobic environment (133, 139) (Fig. 8). Residue Phe112 is critical for the displacement of 5,6-dimethylbenzimidazole from its coordination bond with the cobalt ion of the ring; mutagenesis studies show an 80% loss of activity (141) (Fig. 8).

The PduGH diol dehydratase reactivase. The PduGH protein is thought to be a DDH reactivase because of its high sequence identity to GDH reactivase (DdrAB) (6). The function of DdrAB is to remove inactive forms of B_{12} from GDH, as described above. Early studies of GDH reported that it is inactivated by its substrate (142, 143). Later, Honda et al. showed that GDH was reactivated by ATP and Mn^{2+} in permeabilized cells (*in situ*) (119), and Mori et al. showed that GDH of *Klebsiella* could be reactivated in permeabilized cells of *E. coli* expressing GDH and two adjacent downstream open reading frames (ORFs) (123). These two ORFs were required for reactivation and were named *ddrA* and *ddrB* (123). In further studies, purified DdrAB was shown to reactivate GDH in the presence of ATP and Mg^{2+}. More recent mechanistic studies have shown that DdrAB reactivates GDH by removal of the damaged cofactor, perhaps by a subunit exchange mechanism (124, 144).

Shell Proteins of the Pdu MCP

The current view is that the shell of the Pdu MCP is composed of eight different proteins, PduA, PduB, PduB′, PduJ, PduK, PduN, PduT, and PduU, and possibly a ninth, PduM (58, 84). PduA, PduB, PduB′, PduJ, PduK, PduT, and PduU have one or more BMC domains and are thought to tile together to form the bulk of the MCP shell, which can be modeled as a mixed protein sheet (11, 58, 82). Based on sequence similarity, the PduN protein is thought to be a pentamer that forms the vertices of the Pdu MCP (75). Evidence indicates PduM is an essential MCP structural protein, but its exact role is uncertain (84). Pores found in the center of BMC domain shell proteins are thought to function in the selective transport of enzyme substrates, products, and cofactors via passive and dynamic mechanisms (63). Proteomics analysis has shown that the major shell proteins of the Pdu MCP are PduA, PduB, PduB′, and PduJ and that the minor shell components are PduK, PduN, PduT, and PduU (82). Deletion of the *pduBB′*, *pduJ*, or *pduN* gene severely impairs MCP formation and results in two phenotypes characteristic of a nonfunctional MCP: (i) propionaldehyde toxicity during growth on 1,2-PD and (ii) faster growth on

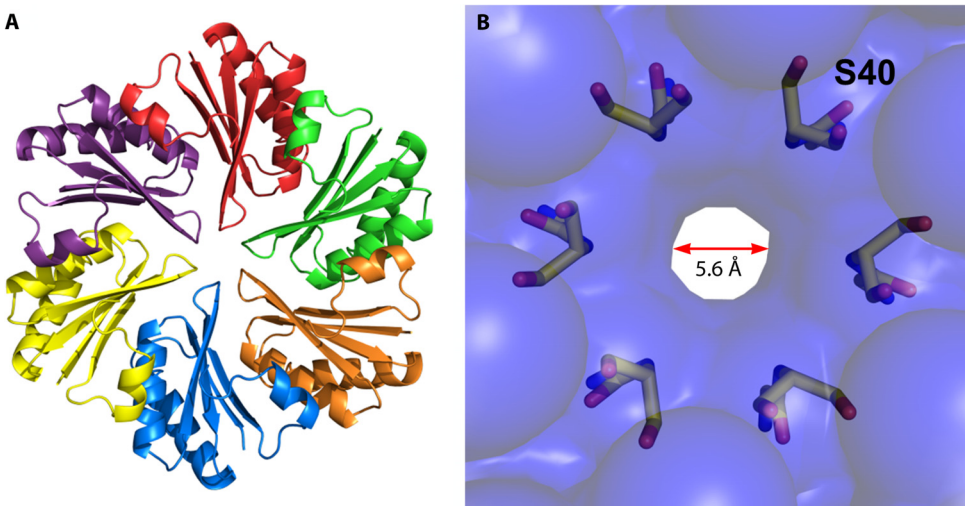

FIG 9 Structure of the PduA shell protein. (A) Hexameric structure of PduA. (B) Surface structure of PduA with pore-lining residues highlighted.

1,2-PD when the B_{12} level is limiting (22, 58). Deletion of the *pduK*, *pduT*, or *pduU* gene did not greatly influence MCP structure or growth on 1,2-PD (58). Strains with a *pduU* or *pduT* deletion do, however, grow slightly slower than the wild type, suggesting that these genes are required for maximal activity of the 1,2-PD degradative enzymes encased within the MCP shell (58). Strains with a *pduA* deletion have intermediate phenotypes. They form larger-than-normal MCPs and are subject to an intermediate level of propionaldehyde toxicity (58). A number of genetic and crystallographic studies of MCP shell proteins have been reported, and these investigations yielded numerous insights into their assembly and function in the Pdu MCP.

PduA is a canonical BMC domain protein. The *pduA* gene encodes a small 94-amino-acid protein which serves as one of the major shell components of the Pdu MCP; it is estimated to comprise 16% of the total shell protein (82). PduA has a single BMC domain and is related to the major carboxysome shell proteins. As evident from immunoelectron microscopy, the PduA protein is a part of the MCP shell (22). Initial studies indicated that a *pduA* deletion mutant of *Salmonella* was unable to produce polyhedral organelles (MCPs) (22). However, more recent studies showed that the initial mutant investigated was in fact a *pduA pduB* double-deletion mutant and that a *pduA* single mutant forms enlarged MCPs with an appearance similar to that of the wild type (58). Nonetheless, *pduA* deletion mutants exhibit phenotypes indicative of damaged MCPs, including growth arrest due to propionaldehyde toxicity and an increased growth rate at limiting B_{12} levels, although these phenotypes are somewhat less severe for *pduA* mutants than for mutants unable to form MCPs (58).

The crystal structure shows that PduA is a symmetric homohexamer (Fig. 9) shaped like a hexagonal disc (68). Adjacent PduA hexamers interact closely to facilitate close packing and thus form a continuous two-dimensional layer without any patencies. This type of molecular layer is formed by a number of MCP shell proteins and is thought to be the basis of MCP shell formation (63).

PduA hexamers have distinct openings along their central axes that are believed to serve as pores for molecular transport across the shell (68). The properties of the PduA pore is suggestive of 1,2-PD transport (68). The pore surface is mostly polar because of the exposed backbone amide nitrogens and carbonyl oxygen atoms of G39 and S40 as well as the side-chain hydroxyl of S40. The diameter of the pore is 5.6 Å, which should occupy 1,2-PD without requiring substantial conformational changes (Fig. 9). The numerous hydrogen bond donors and acceptors in the PduA pore could bind the two hydroxyl groups of 1,2-PD, facilitating transport. On the other hand, propionaldehyde is more hydrophobic than 1,2-PD and presents only a single hydrogen bond acceptor and no donors, potentially limiting the speed of its efflux from the MCP (68).

The PduJ shell protein is closely related to PduA in sequence but is functionally divergent. The PduJ protein shares 80% amino acid sequence identity with PduA, has similar pore-lining residues, and is presumed to have a similar architecture, although its structure has not yet been reported (68). PduJ comprises about 22% of the MCP shell, and in contrast to *pduA*, a *pduJ* deletion mutant forms elongated MCPs (58). This elongated phenotype suggests improper closure of the MCP; hence, PduJ may form the edges that join the MCP facets at the proper angle for closure (58). Strains with a deletion of the *pduJ* gene have phenotypes associated with a nonfunctional MCP, as described above (58).

The PduBB′ proteins may form a gated pore. Havemann et al. identified the *pduB* gene of *Salmonella* by sequence analysis (22). Subsequent proteomics showed that *pduB* is in fact two overlapping genes that are expressed in the same reading frame to produce the PduB and PduB′ proteins (82). PduB and PduB′ are identical in amino acid sequence except that PduB is 37 amino acids longer than PduB′. Further studies in *Citrobacter* showed that PduB and PduB′ are produced from alternative start sites (60). Genetic tests showed that *pduBB′* deletion mutants are unable to form MCPs. EM found that most mutant cells have polar inclusion bodies consisting of aggregated MCP components (Fig. 10) (58). As expected, *pduB* mutants are subject to aldehyde toxicity during growth on 1,2-PD, indicating that the MCP is no longer functional (58).

PduB and PduB′ together comprise over 50% of the total shell protein of the Pdu MCP, 27% and 25%, respectively. Both PduB and PduB′ have two tandem BMC domains and are related to BMC domain proteins proposed to form gated pores in the MCP

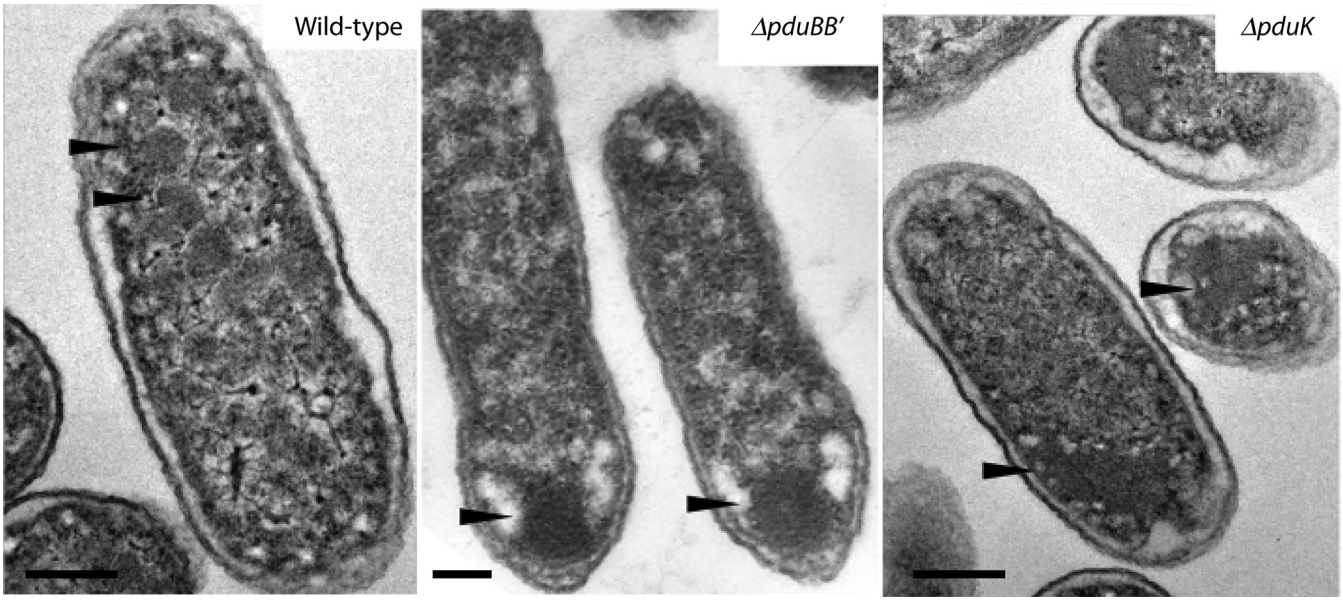

FIG 10 Electron micrographs of mutants impaired for formation of the Pdu microcompartment. The arrows mark normal microcompartments in wild-type *S. enterica*, polar bodies in the Δ*pduBB′* mutant, and aggregated microcompartments in the Δ*pduK* mutant. (Reprinted from reference 58.)

shell (66, 76). The structure of PduB or PduB′ has not been reported for *Salmonella*. However, a crystal structure of the *Lactococcus* PduB protein forms trimers shaped like flat hexagons similar to hexameric BMC domain proteins (77). Like a number of other BMC domain proteins, PduB forms extended two-dimensional sheets in crystals. However, the edge contacts between PduB monomers are slightly out of register compared to other BMC domain proteins, which might lower sheet stability (77). Modeling suggests that PduB and PduA can tile together into a mixed sheet where the edges precisely align, resulting in greater stability (Fig. 11), and this arrangement was suggested to be physiologically important, although it is not yet supported by experimental evidence (77).

The PduK shell protein has a C-terminal domain of unknown function. The PduK protein is 160 amino acids in length. It consists of an N-terminal BMC domain that has a fairly long C-terminal extension (~70 amino acids). It is evident that PduK contains a recognizable [Fe-S] cluster binding motif in its C-terminal domain (CNLCLDPKCPRQKGEPRTLC; cysteine residues that presumably form an Fe-S cluster are underlined) from residue positions 132 to 151. In addition, purified PduK was found to bind iron, supporting the presence of an iron-sulfur center (68). This raises the possibility that PduK functions in electron transfer reactions (68). However, further studies are needed to test this possibility. The structure of PduK has not yet been determined. Genetic analysis showed that a PduK deletion mutation does not impair MCP function but does cause its aggregation (58) (Fig. 10). On this basis, it was proposed that PduK has a role in segregation at cell division (58).

The PduT shell protein has an Fe-S cluster in place of a central pore. PduT is a 184-residue-long tandem-BMC-domain shell protein that assembles as a pseudohexameric homotrimer (68). PduT accounts for about 3% of the total shell protein of the Pdu MCP (82). In crystals, PduT does not form the extended two-dimensional layers seen for several other BMC domain proteins (68). Interactions between the hexamer edges bury only about half as much surface area compared to PduA; this may serve to control the incorporation of PduT, which is a minor shell component. Interestingly, the crystal structure of PduT also revealed a site at the central pore for binding a [4Fe-4S] cluster (68, 78). The ligands for the metal cluster include three cysteine residues (C38), one from each subunit of the trimer, that are located on the con-

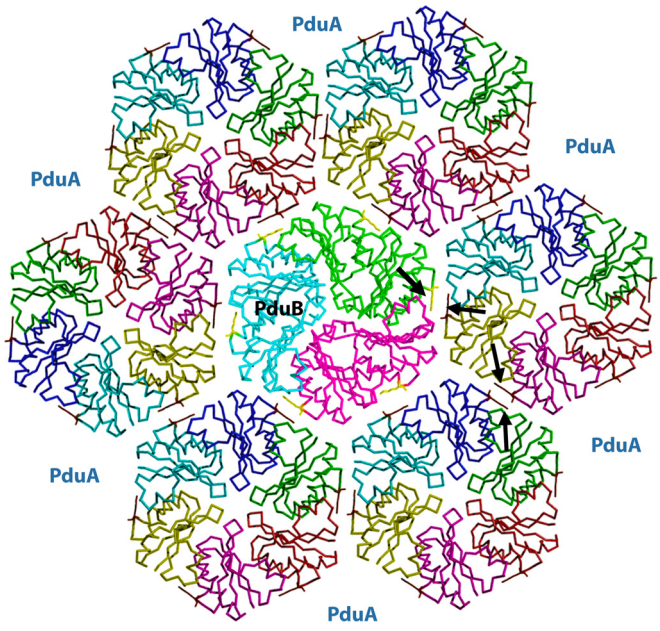

FIG 11 Structure of PduB from *Lactobacillus reuteri*. Modeling indicates that coassembly of PduB and PduA mosaics helps promote stable edge interactions. In this model, a PduB trimer (center) is surrounded by six PduA hexamers. This arrangement brings lysine residues at the edges into register for favorable contacts (arrows).

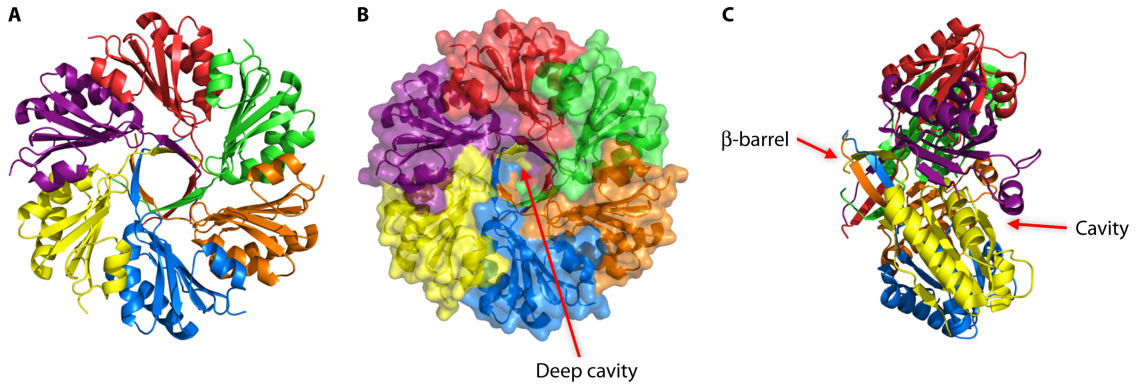

FIG 12 The PduU shell protein is a circularly permutated hexamer whose central pore is capped by a β-barrel. (A) Ribbon model of PduU; (B) surface structure showing a deep cavity on one face of PduU; (C) side view showing a β-barrel that caps the central pore.

served loop at the centermost position of the pore, but the fourth ligand to the iron was not identified (68). It is expected to be positioned transverse to the pore and could extend into the cytoplasm or luminal side of the MCP. It is notable that the [4Fe-4S] cluster is readily accessible from both sides, suggesting a role in electron transfer across the shell or in rebuilding Fe-S centers within the MCP lumen (68). Moreover, PduT contains two more cysteine residues (C108 and C136) in domain II in close proximity, which may form a disulfide linkage. The formation of this disulfide bond might alter the conformation of PduT, resulting in a redox-sensitive change in its pore function (68). In this regard, recent studies by Cheng and Bobik showed that the PduS cobalamin reductase is a component of the Pdu MCP (80). Hence, the putative electron transport function of PduT could be used to support the PduS B_{12} reductase, which mediates a one-electron reduction of the central cobalt atom of B_{12} (80, 106). Alternatively, PduT might be used to rebuild the Fe-S centers of PduS following oxidative damage (80). Genetic tests showed that mutations in PduT only marginally impair growth on 1,2-PD and do not significantly affect MCP structure or function (80). This suggests that the function of PduT might be most important under specific growth conditions not yet identified.

The PduU shell protein has a pore capped by a β-barrel. PduU is a single-BMC-domain protein with a circularly permuted BMC fold (69). It does not form well-packed hexagonal layers in crystals. Instead, PduU has a tendency to form strips of side-by-side hexamers, which may reflect that it is a minor MCP component (Fig. 12). PduU is unique among shell proteins in having an unusual, six-stranded, parallel β-barrel capping the central pore region (Fig. 12C) (69). Typical β-barrels are comprised of larger numbers of β-strands, although a similarly small β-barrel was recently reported in an amyloid peptide (145). When they appear in transmembrane proteins, they are usually comprised of 12 strands or more, thereby creating pores for molecular transport (146). The center of the PduU β-barrel is occluded and unlikely to play a role in transport. It could instead present a specific enzyme binding site. PduU is also unusual in having a deep cavity or depression on the face of the hexamer opposite the β-barrel (69). The surface of this cavity presents several hydrophobic residues, hinting at unknown molecular interactions.

The PduN protein is homologous to pentamers that form MCP vertices. PduN is homologous to pentameric BMV proteins such as CcmL (62). BMV proteins are proposed to form the vertices of bacterial MCPs and aid in their closure (62). Mutants lacking PduN form grossly abnormal MCPs and are subject to propionaldehyde toxicity during growth on 1,2-PD (58). PduN was detected in purified Pdu MCPs by Western blotting. It was also found to be associated with the Pdu MCP of *Citrobacter* by GFP labeling experiments (48). PduN was not detected by Coomassie staining of protein gels due to low abundance (82). This is expected, since there are only 12 vertices in an icosahedron.

The PduM protein is required for MCP formation, but its exact role is uncertain. The PduM protein is required for the formation of the Pdu MCP, but it has no BMC or BMV domain and lacks recognizable sequence similarity to any protein of known function (84). PduM is 163 amino acids in length, and its structure has not yet been determined. Electron microscopy of *pduM* deletion mutants found MCPs that are grossly abnormal in shape along with amorphous cytoplasmic aggregates (84) (Fig. 13). Strains with *pduM* deletion mutations have phenotypes characteristic of a nonfunctional MCP (84).

Other Pdu Enzymes

The PduV GTPase may be involved in MCP segregation at cell division. PduV is a protein of unknown function related to the AAA family of ATPases (17). Indeed, recent observations indicate that purified PduV has weak GTPase activity (48). In addition, GFP fusion analyses suggest that PduV is localized at the outer surface of the microcompartment (48). Interestingly, PduV is proposed to play a role in regulating the spatial distribution of microcompartments within the growing bacterial cell (48). Live-imaging techniques indicate that the movement of the Pdu MCP within the cytoplasm requires the presence of PduV (48). Thus, it can be speculated that PduV might interact with cytoskeletal filaments. However, further studies are required to verify the function of PduV.

PduX is an L-threonine kinase used for B_{12} synthesis. Fan and Bobik showed that the PduX enzyme of *Salmonella enterica* is an L-threonine kinase used for the *de novo* synthesis of Ado-B_{12} and the assimilation of cobyric acid (Cby). PduX converts L-threonine plus ATP to L-threonine-phosphate plus ADP (147). L-Threonine-phosphate is a precursor for the nucleotide loop of Ado-B_{12}. Genetic tests showed that *pduX* mutants were impaired in the synthesis of Ado-B_{12} from cobyric acid and in the *de novo* synthesis of Ado-B_{12} (147). A recombinant PduX enzyme was purified and shown to have L-threonine kinase activity (148). PduX was the

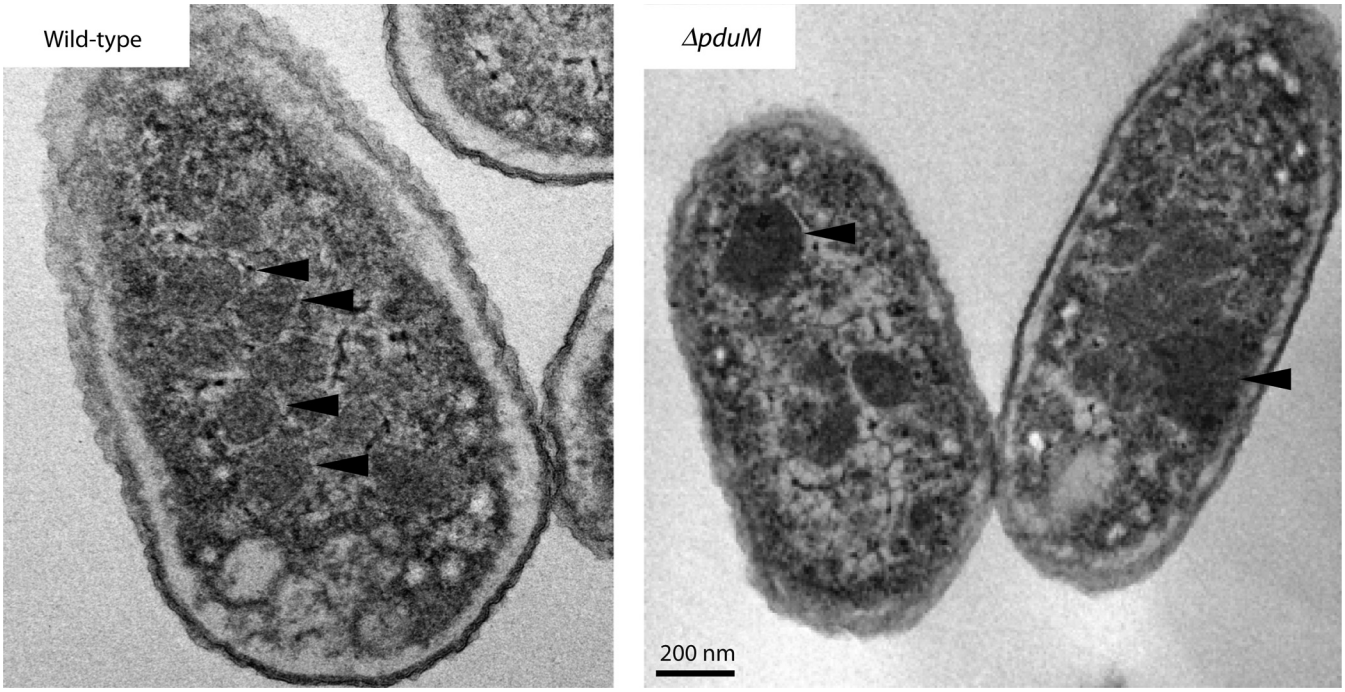

FIG 13 Comparison of wild-type microcompartments of *S. enterica* to those of a Δ*pduM* mutant. (A) Wild-type *S. enterica*; (B) Δ*pduM* deletion mutants. (Reprinted from reference 84.)

first enzyme identified that phosphorylates free L-threonine (147, 148). Further studies of PduX indicate an ordered mechanism in which ATP is the first substrate to bind, and mutation analysis identified several key catalytic residues (148). The role of the PduX enzyme in 1,2-PD degradation is to help provide Ado-B_{12} for DDH (148).

In *Lactobacillus*, the Pdu MCP Is Likely Used for 1,2-PD and Glycerol Degradation as Well as Reuterin Production

Lactobacillus reuteri has a gene cluster closely related to the *pdu* operon of *Salmonella*, which includes genes for 1,2-PD degradation and MCP formation (149). Studies have shown that *L. reuteri* forms a Pdu MCP used for the catabolism of 1,2-PD, as described above, as well as for the metabolism of glycerol (149). Glycerol is metabolized to 3-hydroxypropionaldehyde (HPA) and then to 1,3-propanediol. Although *L. reuteri* does not grow on glycerol as a sole carbon source, added glycerol improves the growth rate and yield during the fermentation of glucose and a variety of other carbohydrates (150). *L. reuteri* is a heterofermentative organism that normally produces lactate, ethanol, and a small amount of acetate during glucose fermentation. Addition of glycerol leaves lactate production essentially unchanged but increases acetate production and decreases ethanol production (150). Furthermore, glycerol supplementation leads to the production of substantial levels of 1,3-propanediol (the product of glycerol dehydration and reduction). These results indicate that HPA (derived from glycerol) serves as an electron acceptor in place of acetyl-phosphate during glucose fermentation, allowing the use of acetyl-phosphate for additional energy generation and thereby increasing the growth rate and yield (150, 151). This is quite different from the situation in *Salmonella*, where glucose and other carbohydrates strongly repress the expression of the *pdu* genes, preventing cofermentation of 1,2-PD (or glycerol) with simple carbohydrates (95, 100). Another interesting aspect of glycerol degradation by *L. reuteri* is that it leads to the production of HPA (also known as reuterin), a broad-spectrum antibiotic associated with the probiotic effects of *L. reuteri* (152, 153). Whole-genome sequence analysis revealed that genes responsible for glycerol degradation are part of the *L. reuteri pdu* operon (154). This operon includes genes with high sequence similarity to the PduCDE diol dehydratase of *Salmonella* (154). Gene knockout studies as well as biochemical investigations confirmed the involvement of the *L. reuteri* PduCDE enzymes in reuterin production (154). The fairly extensive literature on *L. reuteri* as a probiotic and the role of reuterin will not be covered in this review.

THE Eut MCP

A variety of bacteria catabolize ethanolamine as a sole source of carbon and nitrogen by a B_{12}-dependent pathway (155–157). The initial step of ethanolamine degradation is its conversion to acetaldehyde and ammonia by ethanolamine ammonia lyase (EutBC). Subsequent to aldehyde formation, the ethanolamine degradative pathway is analogous to that for 1,2-PD degradation. Like 1,2-PD degradation, ethanolamine utilization involves a bacterial MCP (Eut MCP). The initial evidence for a Eut MCP was the finding that the genes for ethanolamine degradation are clustered with genes encoding MCP shell proteins in *Salmonella* (5, 7). Subsequent studies by Shively et al. showed that *Salmonella* forms MCPs during growth on ethanolamine (158). Similar to the Pdu MCP, the Eut MCP is polyhedral, and its shell is composed primarily of BMC domain proteins (EutK, EutM, EutS, and EutL) and a pentamer (EutN) that forms the vertices of the shell (7, 76). The Eut MCP has been proposed to improve process efficiency while protecting cells from acetaldehyde toxicity (21, 23). However, recent

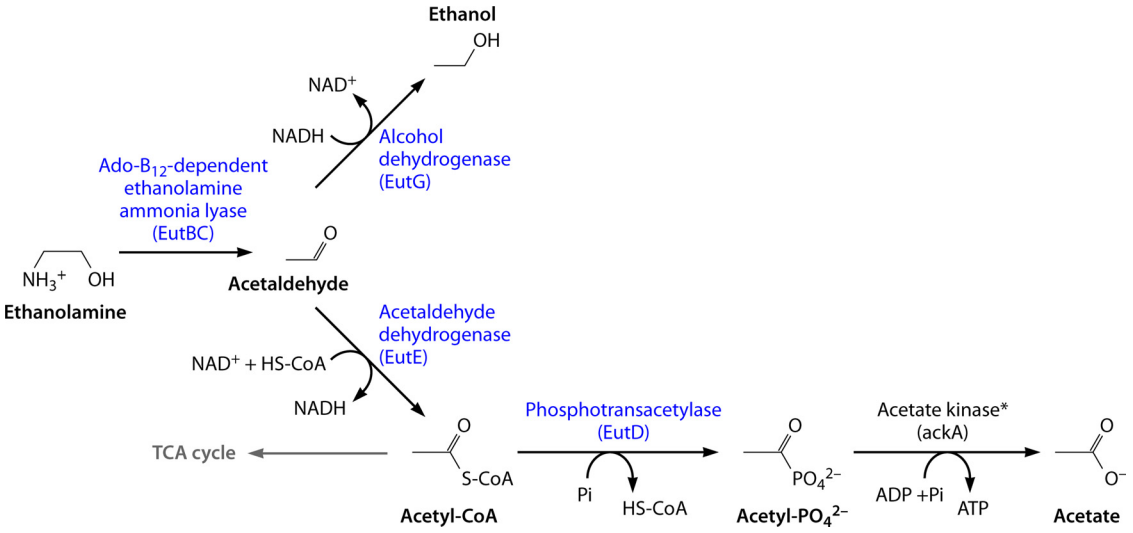

FIG 14 Pathway of coenzyme B_{12}-dependent ethanolamine utilization. Ethanolamine degradation proceeds by a pathway analogous to that of 1,2-PD degradation (Fig. 3), the main difference being C_2 intermediates rather than C_3. As is the case for 1,2-PD degradation, the fermentation of ethanolamine provides a source of ATP and reducing power (NADH) but no source of cell carbon. Under aerobic conditions or during anaerobic respiration with tetrathionate, acetyl-CoA feeds into the TCA cycle to provide additional ATP and biosynthetic building blocks. *, the acetate kinase used for ethanolamine degradation is a housekeeping enzyme encoded outside the *eut* operon.

studies indicate that the main role of the Eut MCP is to prevent the loss of a volatile metabolite (acetaldehyde) through the cell membrane (21). The latter model is supported by extensive genetic tests showing that *Salmonella* mutants unable to make the Eut MCP cannot grow due to carbon loss (21).

Ecology of Ethanolamine Degradation

Genomic analyses indicate that a number of bacteria, including *Actinobacteria*, *Proteobacteria*, *Enterococcus*, *Erwinia*, *Flavobacterium*, *Klebsiella*, *Mycobacterium*, *Pseudomonas*, *Achromobacter*, *Corynebacterium*, *Clostridium*, *Arthrobacter*, *Escherichia*, as well as several other pathogens that cause food poisoning, use an MCP for the B_{12}-dependent degradation of ethanolamine, which can serve as a sole source of both carbon and nitrogen (157). Ethanolamine is a by-product of phosphodiesterase-mediated breakdown of phosphatidylethanolamine, which is a major component of cell membranes in both bacteria and mammals. Hence, ethanolamine is thought to be an important carbon and nitrogen source in diverse environments, including the mammalian gut, where ethanolamine is derived from the host diet as well as bacterial and intestinal epithelial cells (159). Indeed, recent studies indicate that the degradation of ethanolamine within the gut provides a substantial growth advantage to *Salmonella* compared to competing flora and thereby promotes its dissemination to new hosts (see above) (30).

Pathway of Ethanolamine Degradation

The pathway of ethanolamine degradation begins with its conversion to ammonia and acetaldehyde by B_{12}-dependent ethanolamine ammonia lyase (Fig. 14) (EutBC) (155). Some acetaldehyde is converted to acetyl-CoA, then to acetyl-phosphate, and then to acetate. This produces one molecule of ATP by substrate-level phosphorylation (7, 160, 161). In addition, some acetaldehyde is converted to ethanol in order to maintain NADH/NAD^+ balance. The enzymes involved in these reactions include acetaldehyde dehydrogenase (EutE), phosphotransacetylase (EutD), ethanol dehydrogenase (EutG), and the housekeeping acetate kinase (AckA), whose gene maps outside the *eut* gene cluster. Under fermentative conditions, *Salmonella* can use ethanolamine as a sole nitrogen source but not as a sole source of carbon and energy, since none of the ethanolamine pathway intermediates can be diverted into biosynthetic reactions under these conditions (38). Ethanolamine degradation does, however, enhance fermentative cell yield (by providing additional ATP) when yeast extract is available to provide biosynthetic intermediates (38). Under aerobic conditions, *Salmonella* uses ethanolamine as a sole carbon and nitrogen source. When oxygen is available, acetyl-CoA is metabolized via the TCA cycle and the glyoxylate shunt (160). Ethanolamine also functions as a sole carbon and energy source for *Salmonella* during anaerobic respiration when tetrathionate is available as a terminal electron acceptor (38). More common terminal electron acceptors for anaerobic respiration, such as nitrate, fumarate, DMSO, and TMAO, have not been shown to support the anaerobic respiration of ethanolamine, but the reason why they are unable to do so remains uncertain. The pathway of ethanolamine degradation in genera other than *Salmonella* is likely to be similar in terms of the reactions involved. However, regulation is known to be variable, and the types of terminal electron acceptors that support ethanolamine respiration might also vary (157, 159).

Genes for Ethanolamine Degradation

In *Salmonella*, the best-studied case, the genes for ethanolamine utilization (*eut*) are located in a single operon located between the *cysA* and *purC* genes (Fig. 15). This operon contains 17 genes: *eutS*, *eutP*, *eutQ*, *eutT*, *eutD*, *eutM*, *eutN*, *eutE*, *eutJ*, *eutG*, *eutH*, *eutA*, *eutB*, *eutC*, *eutL*, *eutK*, and *eutR* (5). Out of these 17 genes, *eutK*, *eutL*, *eutM*, *eutN*, and *eutS* encode structural proteins that make up the outer shell of the Eut MCP (7, 76). The *eutB* and *eutC* genes encode B_{12}-dependent ethanolamine ammonia lyase (EAL), which breaks down ethanolamine into acetaldehyde and ammo-

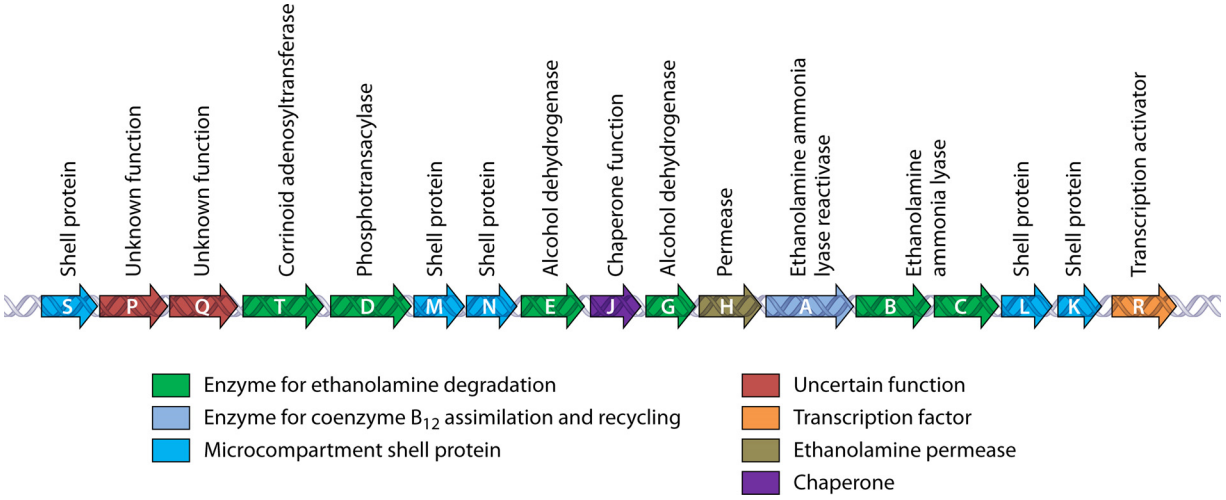

FIG 15 The ethanolamine utilization (*eut*) operon of *S. enterica*. The genes for ethanolamine degradation are found at a single locus that encodes both pathway enzymes and the proteins used to build the Eut MCP.

nia (161). The *eutA* gene encodes an EAL reactivase (162), and the *eutT* gene encodes a corrinoid cobalamin adenosyltransferase that converts cob(I)alamin to Ado-B_{12}, the required cofactor of EAL (163–165). The genes used for the metabolism of acetaldehyde include *eutE*, which encodes an aldehyde dehydrogenase that converts acetaldehyde plus HS-CoA plus NAD^+ to acetyl-CoA plus NADH (7, 161). Subsequently, acetyl-CoA is converted into acetate by the sequential action of a phosphotransacetylase encoded by *eutD* and a housekeeping acetate kinase (*ackA*) encoded outside the *eut* operon (7, 161). The *eutH* gene encodes a transport protein for ethanolamine that is most important at low pH (166). The *eutJ* gene is proposed to encode a chaperone whose specific function is currently unknown (7). The functions of *eutP* and *eutQ* are also unknown, although EutP shares sequence similarity to GTPases (7). Lastly, the *eutR* gene encodes a positive regulatory protein required for induction of transcription of the *eut* operon (167, 168). Genomic studies indicate that there is some variation in the structures of Eut operons among different phyla (157, 159). In most cases, the genes that encode B_{12}-dependent ethanolamine lyase (*eutBC*), the key enzyme of ethanolamine degradation, are associated with proteins for MCP formation (159). Within such operons, there is some variation in the number of types of MCP genes present, likely reflecting divergence in the details of MCP construction. In some cases, however, *eutBC* genes are found in genomes that lack MCP-specific proteins. For these organisms, an alternative method for mitigating acetaldehyde toxicity/volatility is implied (159).

Regulation of the *eut* Operon

As is the case for other aspects of ethanolamine utilization, the regulation of the *eut* operon is best understood in *Salmonella*. In *Salmonella*, regulation of the *eut* operon is unusual in two respects: (i) a positive transcriptional regulator (EutR) is encoded within the *eut* operon at its downstream end, and (ii) induction of the *eut* operon by the EutR protein requires the simultaneous presence of two effectors, ethanolamine and Ado-B_{12} (167, 168). Because the *eutR* gene is located within the *eut* operon, autoinduction occurs and is required for maximal operon expression. Placement of the *eutR* gene within the operon is thought to help balance competition between EAL and the EutR regulatory protein for a limited amount of Ado-B_{12} (168). At the global level, the *eut* operon is regulated by the cAMP-CRP system; hence, induction requires growth on poor carbon sources (167, 168).

In organisms other than *Salmonella*, alternative strategies are used for *eut* operon regulation (159). *Enterococcus faecalis* uses a two-component sensor kinase (EutW) in conjunction with a response regulator (EutV) that has an RNA binding motif suggested to control expression by antitermination (169). In addition, *Enterococcus* uses an intercistronic Ado-B_{12}-sensitive riboswitch as a second layer of control (169). Based on comparative genomics, this multilayer circuit is also present in *Clostridium* and *Listeria* species.

The Eut MCP Functions To Minimize the Loss of a Volatile Metabolic Intermediate, Acetaldehyde

The Eut MCP includes at least five MCP shell proteins, EutK, EutL, EutM, EutN, and EutS (7). Genetic studies have shown that EutK, EutL, EutM, and EutN are indispensable for the growth of *Salmonella* on ethanolamine under conditions that promote the volatilization of acetaldehyde (21). Mutations in the *eutK*, *eutL*, *eutM*, and *eutN* genes disrupt the shell of the MCP, resulting in acetaldehyde leakage to an extent that prevents growth due to carbon loss (21). Other studies have suggested that acetaldehyde toxicity may also be important. Genetic tests showed that *polA* (DNA repair polymerase) and *gsh* (glutathione biosynthesis) mutants are unable to grow on ethanolamine, and aldehyde toxicity was proposed to account for these phenotypes (23, 102). Potential toxic effects of acetaldehyde have also been proposed based on analogy with the Pdu MCP, whose primary role is mitigation of propionaldehyde toxicity (5). Given the much higher vapor pressure of acetaldehyde than of propionaldehyde, carbon loss due to volatility is likely to be more significant in the *eut* system than in the *pdu* system.

Shell Proteins of the Eut MCP

The EutM shell protein is a canonical BMC domain hexamer. EutM is a flat cyclic hexameric protein with the α/β fold characteristic of the MCP shell proteins that form extended sheets. It is a

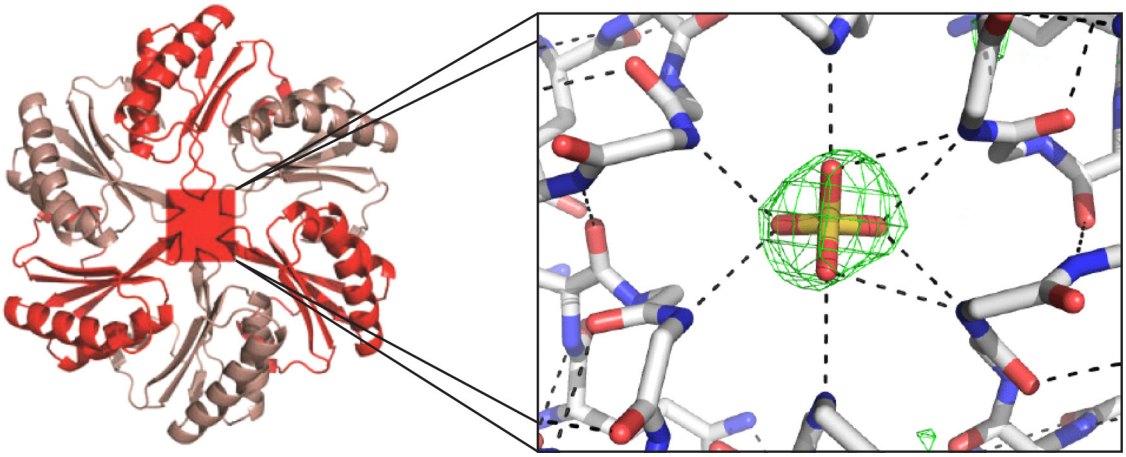

FIG 16 Hexameric structure of EutM. EutM is a good candidate for a major shell protein of the Eut MCP. Its central pore is occupied by a sulfate ion, consistent with a role as a molecular conduit for small molecules. (Reprinted from reference 76 with permission from AAAS.)

97-amino-acid-long protein whose structure has been determined at a resolution of 2.1 Å (76). In the crystal structure, the central pore in the EutM hexamer was occupied with a sulfate ion (from the crystallization buffer), which is consistent with the idea that such pores can be used as conduits for ions and small molecules (Fig. 16). Because EutM has structural features typical of MCP shell proteins, it is a good candidate for a major building block of the Eut MCP (76). In contrast, other BMC domain proteins encoded by the *eut* operon were found to have unusual structural features, suggesting specialized functional roles, as further described below (76).

EutL is a pseudohexameric trimer that may serve as a gated pore for metabolite transport. EutL is the largest BMC domain protein in the Eut MCP system (76). An interesting feature of this protein is that each monomer is a combination of two tandem, circularly permuted BMC domains (65, 76). Consequently, the ultimate tertiary structure of the trimeric protein is a pseudohexamer similar in overall shape to canonical BMC domain hexamers. Another unique feature of EutL is that it appears to have a gated pore at the center of the trimer (Fig. 17) (76). The idea of a gated pore is based on crystal structures that revealed pore-open and pore-closed conformers (76). Comparison of these conformers suggests that there are substantial movements (~15 Å) in the loop residues (residues 65 to 83 and 174 to 185) during interconversion of the two forms. The open pore is triangular, with edges of ~11 Å in length, and the narrowest part of the pore has a diameter of ~8 Å, which is large enough for the transport of enzymatic cofactors. Presumably, a cofactor could bind the closed pore, which would open, allow the factor into the MCP, and then close. In addition, EutL was also found to crystallize in molecular layers, suggesting that it is present as a major structural component of the Eut MCP shell (65, 76).

The EutS shell protein is a bent hexamer. EutS is a 111-amino-acid-long shell protein that adopts the typical α/β fold of the BMC domain proteins (76). The crystal structure of the EutS hexamer has been reported at a 1.65-Å resolution (76). The primary amino acid sequence of EutS is circularly permuted with reference to the sequences of other BMC domain proteins. The structure of EutS is also quite different from that of the canonical BMC domain proteins. Typical BMC domain proteins form flat hexameric struc-

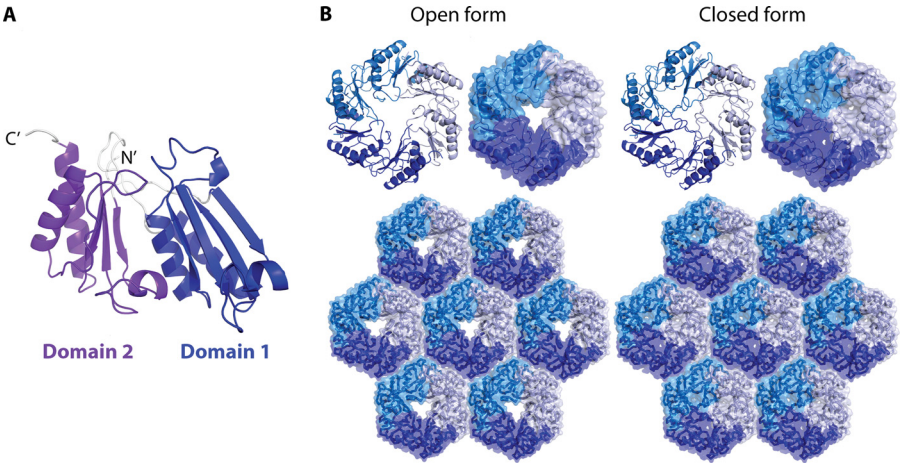

FIG 17 The structure of the EutL shell protein suggests a gated pore to control the movement of metabolites from the cytoplasm to the MCP lumen. (A) EutL monomer in its closed form. (B) Open and closed configurations of EutL trimers in both ribbon diagram and surface representations. EutL forms extended protein sheets, as do a number of other MCP shell proteins (bottom). (Reprinted from reference 76 with permission from AAAS.)

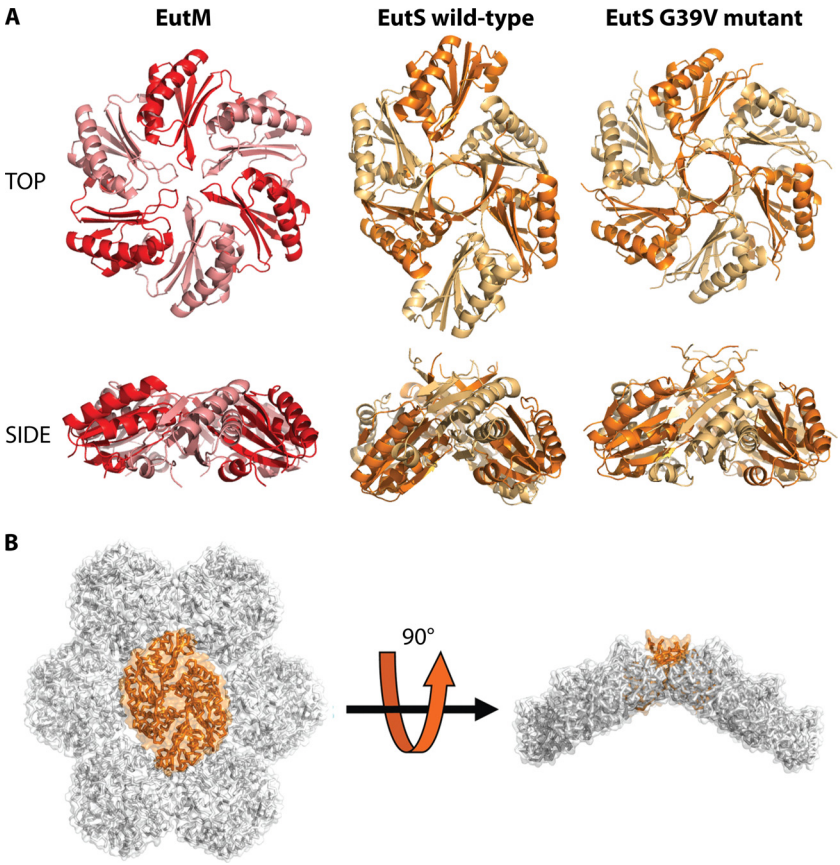

FIG 18 Comparison of the structures of the EutS and EutM shell protein hexamers. (A) EutM, wild-type EutS, and the EutS G39V mutant shown in two views. The wild-type EutS hexamer is bent away from a flat configuration by approximately 40°. The EutS G39V mutant is flat. (B) Hypothetical model showing how EutS (orange) might introduce curvature in an otherwise flat hexameric sheet of shell protein hexamers. (Reprinted from reference 76 with permission from AAAS.)

tures. In contrast, the EutS hexamer has a bend of ~40° (Fig. 18). Due to this bend, the EutS protein is proposed to form the edges that join the facets of the Eut MCP (76). Interestingly, based on sequence analysis, a EutS G39V mutant was constructed and was found to form a flattened symmetrical hexamer similar to that of the canonical BMC domain proteins when crystallized (Fig. 18). Moreover, further investigation revealed that G39 is conserved among EutS proteins (encoded in the *eut* operons of other bacteria) but is absent from other BMC proteins. Thus, a subtle change may have allowed functional diversification of the EutS protein.

The EutK shell protein has a C-terminal nucleic acid binding domain. EutK is an exceptional protein in the Eut MCP system. While all other shell proteins are reported to be oligomeric (trimeric or hexameric) in nature, EutK was found to be monomeric in solution (76). Moreover, in addition to the conserved BMC domain, EutK has a 60-amino-acid C-terminal extension following the BMC domain. Although the crystal structure of the full-length EutK protein has not been reported, that of the 60-amino-acid extension was solved and shown to contain a helix-turn-helix motif typical of nucleic acid binding proteins (76). Moreover, this structure has a localized high positive charge, further supporting its role in DNA/RNA binding. However, as yet, its exact functional role is unknown.

The EutN shell protein is a pentamer. EutN is not a BMC domain protein. Rather, it has sequence similarity to CcmL and CsoS4A, which are pentameric vertex proteins in carboxysomes. Initially, the structure of EutN from *E. coli* was reported as a hexamer at a resolution of 2.7 Å (74). It was then suggested that EutN might distort to fit in the vertices of the Eut MCP and that this distortion could account for the irregular polyhedral shape of Eut MCPs compared to the nearly icosahedral structure of carboxysomes (74). However, a recent report unequivocally demonstrated that EutN is primarily a pentamer in solution by using a technique called oligomeric characterization by addition of charge (9). A comparison of conditions used to obtain crystals of EutN and those of the solution state experiments offered no clear explanation for the observed difference between crystalline and solution oligomer states. The hexameric form of EutN may have been a minor species that selectively crystallized, although the possibility that EutN polymorphism is important in the Eut MCP cannot be discounted.

DIVERSE MICROCOMPARTMENTS

Protein database searches indicate that about 16% of bacterial species have MCP gene clusters that consist of enzyme-encoding genes interspersed with genes for MCP shell proteins (13, 15, 17, 18, 20, 170). The α- and β-carboxysomes (16) as well as the Pdu and Eut MCPs described above represent the best-characterized MCP types. In addition, recent studies have identified an MCP for degradation of plant saccharides that may be limited to the *Verrucomicrobia* and *Planctomycetes* (27). Beyond these MCPs, three

additional types of MCPs have been identified computationally, and several variants representing apparent functional embellishments on the well-characterized MCP types have been highlighted as well (9, 15). Based on bioinformatic analyses, these three lesser-studied MCPs are proposed to function in ethanol metabolism during ethanol/acetate fermentation (Etu MCP), 1,2-PD degradation by a B_{12}-independent pathway that involves a glycyl radical enzyme (Grp MCP), and amino alcohol utilization (9). These three types as well as the recently identified MCP involved in plant saccharide breakdown are described further below. For more details on the carboxysome MCP, the reader is referred to excellent recent reviews (13, 16).

The Grp MCP for B_{12}-Independent 1,2-Propanediol Degradation

The *grp* operon is proposed to mediate the degradation of 1,2-PD (or possibly glycerol) by using a glycyl radical enzyme that is B_{12} independent, rather than the more common B_{12}-dependent enzyme (9). Operons of the *grp* type characteristically contain four enzymes that are interspersed with MCP shell genes (9). The four core enzymes common to *grp* operons include a glycyl radical diol dehydratase that has sequence similarity to pyruvate formate lyase, glycyl radical activase (*S*-adenosylmethionine synthase), aldehyde dehydrogenase, and a putative chaperone. Based on the presence of these enzymes, the Grp MCP is proposed to mediate 1,2-PD degradation by a pathway similar to that used by the Pdu MCP, except that the first reaction (the conversion of 1,2-PD to propionaldehyde) is mediated by a glycyl radical enzyme rather than the B_{12}-dependent diol dehydratase (9). A role for *grp* in 1,2-PD degradation is further supported by microarray studies that showed *grp* operon induction in response to fucose, a common methylpentose that is broken down via 1,2-PD (171). Nonetheless, *grp* operons might also function in glycerol degradation, since the glycyl radical enzyme found in these systems is also active with glycerol (172, 173). Most likely, a Grp MCP would be involved in the use of glycerol as a hydrogen acceptor, as described above for *L. reuteri*, since the enzymes associated with the fermentation of glycerol via dihydroxyacetone are absent from *grp* gene clusters. However, as yet, a role for *grp* genes in glycerol degradation is not supported by physiological studies.

An interesting aspect of the Grp MCPs is that they appear to be elaborated as several diversified subclasses (9). Grp operons that contain only the common enzymatic core (the four enzymes described above) together with MCP proteins are conserved across >20 species, indicating a broad distribution in nature (9). A second type of Grp MCP gene cluster encodes two proteins in addition to this core: one has homology to the C terminus of PduO (a domain of unknown function that is part of the PduO adenosyltransferase), and another has similarity to a macrophage inflammatory channel protein known to transport small neutral metabolites across the membrane. The latter protein might be involved in the transport of metabolites across the shell in the Grp MCPs, but as yet, there is no experimental evidence to support this idea. A third subclass of Grp MCP operon encodes two drug resistance proteins, two regulatory proteins, and a phosphotransacylase that is a homolog of PduL from the Pdu MCP system (89). The PduL-type phosphotransacylase is expected to function in the predicted pathway of 1,2-PD degradation and may be a substitute for an analogous housekeeping enzyme used in other Grp systems. The roles of the drug resistance proteins within the context of the Grp MCP are unclear, and the distinctive regulatory proteins suggest a divergent control system. Another *grp* gene cluster encodes two regulatory proteins similar to a histidine kinase sensor and a response regulator receiver present in the *eut* operon. These clusters likely represent a third type of regulatory system for *grp* gene expression that may be similar to that found in some Eut systems (see above) (159, 169). Yet another variation on the *grp* MCP might include enzymes for later steps of rhamnose and fucose degradation. Both rhamnose and fucose are fermented via 1,2-PD, and some *grp* gene clusters encode homologs of fuculose and rhamnulose aldolase that are induced by these methylpentoses (171, 174).

Shell Proteins of the Grp MCP

The gene clusters for the Grp MCPs have at least four paralogs of genes that encode hexameric/pseudohexameric BMC domain shell proteins (9). In addition, they also contain a gene encoding a pentameric vertex protein (75). A distinctive feature of the Grp MCPs in *Desulfovibrio salexigens* and *Desulfovibrio desulfuricans* is they have up to three different tandem-BMC-domain shell proteins, suggesting divergent functional requirements. Also of interest is an unusual Grp shell protein from *Pectobacterium wasabiae* (Pecwa_4094). UV-visible (UV-Vis) spectroscopy of purified Pecwa_4094 indicates an iron-sulfur cluster, which would be the first such cluster present in a single-BMC-domain protein (9). Overall, the shell of the Grp MCP appears to have a number of intriguing functional variations that may provide insight into MCP evolution and diversification.

Amino Alcohol Degradation May Occur within an MCP in Some Species

Bioinformatic studies identified a presumptive MCP in at least four organisms, *viz.*, *Mycobacterium smegmatis*, *Mycobacterium* sp. strain MCS, *Mycobacterium gilvum*, and *Mycobacterium vanbaalenii* (but not *Mycobacterium tuberculosis*), that may be involved in the metabolism of amino alcohols (9). The operons identified in these organisms encode two BMC shell proteins as well as a putative vertex protein (9). Two enzymes found in these operons are similar to enzymes used for 1-amino-2-propanol metabolism, and others include a class III aminotransferase, an amino acid permease-associated protein, and an aminoglycoside phosphotransferase (9). Hence, an MCP involved in amino alcohol metabolism was proposed.

MCP for Ethanol/Acetate Fermentation (Etu MCP)

Seedorf and coworkers proposed that an MCP is involved in the fermentation of ethanol/acetate by *Clostridium kluyveri* (175). In *C. kluyveri*, MCP shell genes are associated with two genes for ethanol metabolism, NAD-dependent ethanol dehydrogenase and NAD(P)-dependent acetaldehyde dehydrogenase (175). In ethanol/acetate fermentation, ethanol is converted to acetyl-CoA via acetaldehyde (reverse direction from the Eut system). Presumably, the MCP would serve to trap acetaldehyde to prevent carbon loss and cellular toxicity. The Etu MCP has been characterized to only a very limited extent. The crystal structure of the EtuB shell proteins was determined at a 3-Å resolution—it is a trimer with pseudohexagonal symmetry (67)—and initial genomic studies suggest that the Etu MCP may be one of the simplest MCPs found in nature, consisting of only two shell proteins and encapsulated enzymes (176, 177).

MCP for Degradation of Plant Saccharides in *Planctomyces*

Recent studies of *Planctomyces limnophilus* identified an MCP used for the degradation of L-fucose, L-rhamnose, and fucoidan (27). This MCP was proposed to function in the detoxification of pathway intermediates formed during the degradation of these sugars. In the case of L-fucose or L-rhamnose, the *P. limnophilus* MCP is proposed to mediate the disproportionation of lactaldehyde (produced from either L-fucose or L-rhamnose) to 1,2-propanediol and lactate (27). Subsequently, lactate would feed into central metabolism to provide carbon and energy for growth. In *P. limnophilus*, there is no evidence for the further degradation of 1,2-propanediol, which is thought to be excreted as a metabolic end product (27).

BIOTECHNOLOGY APPLICATIONS OF BACTERIAL MCPs

MCPs as Bionanoreactors for *In Vivo* Pathway Optimization

A primary goal of metabolic engineering is the design of reaction pathways for the high-level production of chemicals and pharmaceuticals. There are several factors, such as diffusion restrictions, alternate metabolic routes, accumulation of toxic intermediates, and inhibitory products, that frequently reduce the efficiency of engineered pathways. In nature, cells may bypass such issues by colocalizing metabolic enzymes in a compartment (176–178). A hallmark example of this strategy can be seen in organelles of eukaryotes such as the peroxisome (179, 180). Using bacteria, the workhouses for industrial chemical production, synthetic biologists have begun to address these difficulties by using scaffolds to organize enzymes. By using scaffolds built from protein or DNA, product yields have been substantially increased for a number of chemicals, including glucaric acid, mevalonate, and resveratrol (181–183). An alternative to scaffolds with several inherent advantages is compartmentalization. Pathway encapsulation would not only increase flux through pathways with poor kinetic properties but also allow control of molecules that enter or exit, sequestration of intermediates, and optimization of the local chemical microenvironment. Several possible compartment platforms have been suggested for both *in vivo* and *in vitro* applications, including viral capsids, lumazine synthase capsids, polymeric cages, liposomes, and bacterial MCPs (184–187). Bacterial MCPs seem particularly well suited for the development of intracellular bioreactors, since evolution has designed MCPs to isolate biochemical reactions with the purpose of regulating enzyme activity, enhancing pathway flux, and protecting cells from toxic intermediates. Indeed, with this in mind, studies aimed at developing the tools to repurpose MCPs are being carried out in an increasing number of laboratories.

Heterologous Expression of Bacterial MCPs

Several groups have conducted studies toward the development of MCPs for biotechnological applications by expressing MCP proteins in *E. coli*. An early advance in recombinant engineering of MCPs was reported by Parsons et al., who expressed several *pdu* genes (*pduA*, *pduB*, *pduJ*, *pduK*, *pduN*, *pduT*, and *pduU*) from *Citrobacter freundii* in *E. coli* to successfully produce empty Pdu MCP shells (60). Here it was found that the minimum number of Pdu MCP shell components required to form a microcompartment was only six proteins (PduA, -B, -B′, -J, -K, and -N). The absence of the remaining Pdu shell proteins PduU and PduT did not prevent formation of the recombinant MCP shells. However, in *Salmonella*, the production of Pdu MCPs requires the PduM protein, and PduA was found to be dispensable (84). Hence, the possibility that there may be some variation in the assembly requirements, even of closely related MCP systems, should be considered. In more recent studies, the *Salmonella pdu* genes were also used to produce synthetic MCPs and compartmentalize specific proteins (188). In these studies, vectors for expression of nonnative cargo proteins were constructed, and Western blots as well as an *in vivo* protease accessibility assay were used to evaluate encapsulation. Recently, a proof-of-concept was done with the Pdu system, where targeting sequences were used to coencapsulate pyruvate decarboxylase and alcohol dehydrogenase within a recombinant shell, leading to increased ethanol production compared to production by strains with unencapsulated enzymes (50). Studies aimed at the production of synthetic MCPs have also been carried out with the Eut system, where empty Eut MCPs were produced in *E. coli* by the expression of the *S. enterica* Eut shell genes *eutK*, *eutL*, *eutM*, *eutN*, and *eutS* (42). Surprisingly, a minimal Eut MCP that was morphologically similar to wild-type Eut MCPs was formed by expression of the EutS protein alone, offering the possibility of a minimal system for biotechnology applications (42). In a very recent study, *E. coli* was used to produce recombinant MCP shells from *Haliangium ochraceum* as well as to target enzymes to these shells (189). A potential advantage of this system for biotechnology applications was the high yield of shells and their uniformity and small size. Also of note is a recently reported flow cytometry system that enables rapid quantitation of protein encapsulation within MCPs (49). This system, which is based on encapsulation conferring proteolytic protection to a fluorescent reporter with a small stable RNA (SSRA) tag, should substantially facilitate the development of optimized targeting systems (49). In another line of investigation, the recombinant production of carboxysomes in *E. coli* was achieved by the expression of no more than 10 genes from *Halothiobacillus neapolitanus*, and the structures formed were very similar to those of the native host (59). This advance provides a synthetic system to drive enhanced CO_2 fixation as well as for fundamental research on carboxysomes (59).

Targeting Heterologous Proteins to Bacterial MCPs

Targeting heterologous proteins for encapsulation is a key step toward utilizing MCPs as customizable nanobioreactors. As described above in this review, N-terminal targeting sequences (of about 18 amino acids in length) have been used to target heterologous proteins, such as GFP, to bacterial MCPs in several instances (40, 42). Mechanistically, MCP targeting sequences are thought to form α-helices that bind to short C-terminal helices of shell proteins, leading to encapsulation during assembly (41). While more work is needed to provide a detailed understanding of this mechanism, results to date suggest that engineering interactions between the tails of shell proteins and lumen enzymes might allow the encapsulation of multiple heterologous proteins within a synthetic shell at defined stoichiometries.

Cargo Delivery by Bacterial MCPs

The application of MCPs as cargo carriers for molecular delivery was discussed recently elsewhere (190). Such cargos could include metal nanoparticles, cytotoxic chemicals, and cytotoxic proteins that are surrounded by a self-assembling protein shell. This strategy would have potential applications for medicinal uses such as tumor imaging and cancer therapy. In cancer therapy, reactive

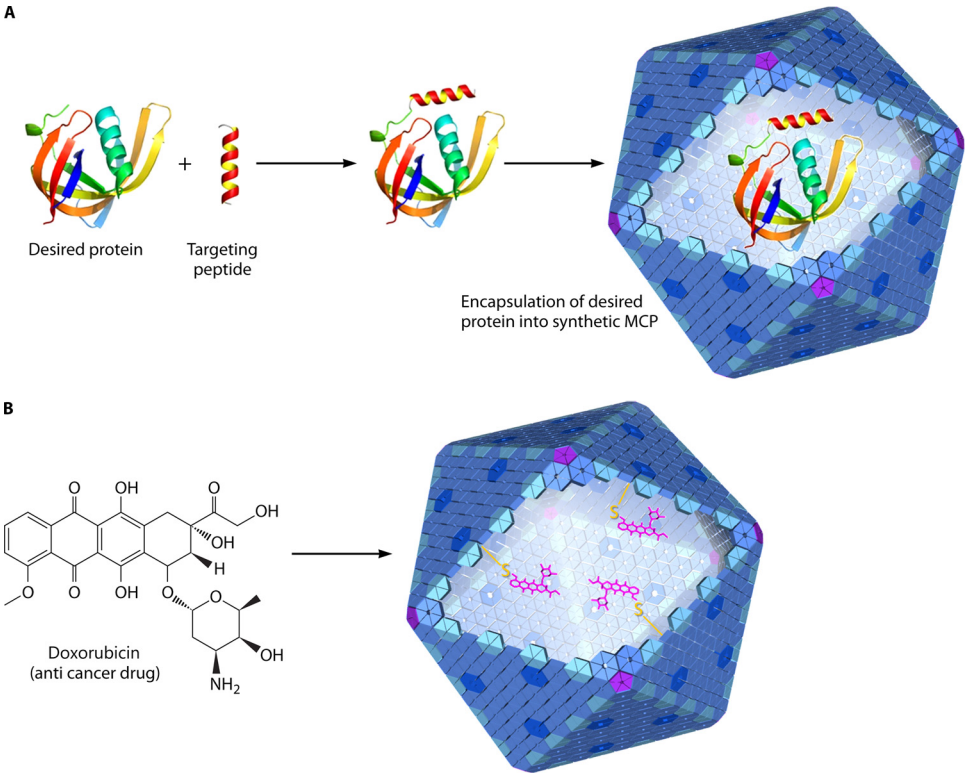

FIG 19 Possible biotechnology applications of bacterial microcompartments. (A) Directing a protein of interest into a synthetic microcompartment might allow engineering of nanobioreactors for chemical production. (B) Bacterial microcompartments as drug delivery vehicles. Doxorubicin, an anticancer drug, might be encapsulated in the lumen of the synthetic microcompartment and targeted to diseased cells.

analogs of anticancer drugs could be chemically attached to thiols on the interior of the MCP surface by engineering cysteine residues at desired positions. In this way, cytotoxic drugs could be sequestered from normal cells while being transported to targeted cancer cells, thereby potentially limiting associated side effects (Fig. 19) (190). A number of potential targeting systems to direct MCPs to disease sites can also be envisioned (190). Chemical tethers such as cysteine residues could be engineered to the MCP surface, followed by chemical linking of a desired small molecule. Alternatively, monoclonal antibodies and recombinant antibody fragments conjugated to the MCP surface are also possible choices (190).

Controlling the Microenvironment within Bacterial MCPs

The shells of bacterial MCPs are made of protein subunits punctuated by pores that are thought to selectively control the entry and egress of small molecules (63). This system, when understood at a fundamental level, could allow precise control over the MCP microenvironment. Pores of desired selectivity could be engineered to allow the entry of desired substrates, sequester key metabolic intermediates, block metabolic branching, improve flux past inefficient enzymes, and selectively allow product exit. However, as yet, the principles of pore function are obscure, and more foundational work is needed to support engineering efforts aimed at building pores with desired selectivity.

CONCLUSIONS

Bacterial MCPs are widespread in nature and functionally diverse. They evolved in bacteria as a means of optimizing metabolic pathways that have toxic or volatile intermediates. MCPs allow metabolic reactions to occur in a unique microenvironment that is bounded by a protein shell rather than a lipid bilayer. The protein shell restricts the diffusion of small polar molecules (CO_2, aldehydes, and perhaps other small polar molecules) that are not effectively retained by a traditional cell envelope based on a lipid bilayer. Although this purpose is simple conceptually, implementation requires an organelle that is 1,000 times larger than a ribosome and that is composed of 10 to 20 different functionally diverse proteins. Works by a number of laboratories employing the varied methods of crystallography, genetics, biochemistry, and cell biology have yielded insights into the underlying principles of bacterial MCPs and provided a basis for the development of engineering tools needed to design purpose-built MCPs. Indeed, many potential applications have been suggested, as described above. However, much of the MCP story still remains to be told before such applications can be practically realized. Key unanswered questions include how pore selectivity is controlled, how multiple shell proteins assemble into an ordered structure with a defined stoichiometry and overall size, the factors that control MCP stability/lifetime, as well as the principles that control the internal organization and activity of encapsulated enzymes. Thus, while we have learned a great deal about bacterial MCPs, many intriguing questions remain to be answered.

ACKNOWLEDGMENTS

This work was supported by grant AI081146 from the National Institutes of Health to T.O.Y. and T.A.B. and by NSF grant MCB0616008 to

T.A.B. S.C. was supported by NRSA GM-0846 and the UCLA Graduate Division.

We thank members of the Bobik and Yeates laboratories for helpful discussions.

REFERENCES

1. **Drews G, Niklowitz W.** 1956. Beiträge zur Cytologie der Blaualgen. II. Zentroplasma und granulare Einschlüsse von *Phormidium uncinatum*. Arch. Mikrobiol. **24:**147–162.
2. **Shively JM, Ball F, Brown DH, Saunders RE.** 1973. Functional organelles in prokaryotes: polyhedral inclusions (carboxysomes) of *Thiobacillus neapolitanus*. Science **182:**584–586. http://dx.doi.org/10.1126/science.182.4112.584.
3. **Cannon GC, Shively JM.** 1983. Characterization of a homogenous preparation of carboxysomes from *Thiobacillus neapolitanus*. Arch. Microbiol. **134:**52–59. http://dx.doi.org/10.1007/BF00429407.
4. **Chen P, Andersson DI, Roth JR.** 1994. The control region of the *pdu/cob* regulon in *Salmonella typhimurium*. J. Bacteriol. **176:**5474–5482.
5. **Stojiljkovic I, Baeumler AJ, Heffron F.** 1995. Ethanolamine utilization in *Salmonella typhimurium*: nucleotide sequence, protein expression, and mutational analysis of the *cchA cchB eutE eutJ eutG eutH* gene cluster. J. Bacteriol. **177:**1357–1366.
6. **Bobik TA, Havemann GD, Busch RJ, Williams DS, Aldrich HC.** 1999. The propanediol utilization (*pdu*) operon of *Salmonella enterica* serovar Typhimurium LT2 includes genes necessary for formation of polyhedral organelles involved in coenzyme B_{12}-dependent 1,2-propanediol degradation. J. Bacteriol. **181:**5967–5975.
7. **Kofoid E, Rappleye C, Stojiljkovic I, Roth J.** 1999. The 17-gene ethanolamine (*eut*) operon of *Salmonella typhimurium* encodes five homologues of carboxysome shell proteins. J. Bacteriol. **181:**5317–5329.
8. **Brinsmade SR, Paldon T, Escalante-Semerena JC.** 2005. Minimal functions and physiological conditions required for growth of *Salmonella enterica* on ethanolamine in the absence of the metabolosome. J. Bacteriol. **187:**8039–8046. http://dx.doi.org/10.1128/JB.187.23.8039-8046.2005.
9. **Jorda J, Lopez D, Wheatley NM, Yeates TO.** 2013. Using comparative genomics to uncover new kinds of protein-based metabolic organelles in bacteria. Protein Sci. **22:**179–195. http://dx.doi.org/10.1002/pro.2196.
10. **Yeates TO, Crowley CS, Tanaka S.** 2010. Bacterial microcompartment organelles: protein shell structure and evolution. Annu. Rev. Biophys. **39:**185–205. http://dx.doi.org/10.1146/annurev.biophys.093008.131418.
11. **Yeates TO, Jorda J, Bobik TA.** 2013. The shells of BMC-type microcompartment organelles in bacteria. J. Mol. Microbiol. Biotechnol. **23:**290–299. http://dx.doi.org/10.1159/000351347.
12. **Yeates TO, Thompson MC, Bobik TA.** 2011. The protein shells of bacterial microcompartment organelles. Curr. Opin. Struct. Biol. **21:**223–231. http://dx.doi.org/10.1016/j.sbi.2011.01.006.
13. **Kerfeld CA, Heinhorst S, Cannon GC.** 2010. Bacterial microcompartments. Annu. Rev. Microbiol. **64:**391–408. http://dx.doi.org/10.1146/annurev.micro.112408.134211.
14. **Kinney JN, Axen SD, Kerfeld CA.** 2011. Comparative analysis of carboxysome shell proteins. Photosynth. Res. **109:**21–32. http://dx.doi.org/10.1007/s11120-011-9624-6.
15. **Bobik TA.** 2006. Polyhedral organelles compartmenting bacterial metabolic processes. Appl. Microbiol. Biotechnol. **70:**517–525. http://dx.doi.org/10.1007/s00253-005-0295-0.
16. **Rae BD, Long BM, Badger MR, Price GD.** 2013. Functions, compositions, and evolution of the two types of carboxysomes: polyhedral microcompartments that facilitate CO_2 fixation in cyanobacteria and some proteobacteria. Microbiol. Mol. Biol. Rev. **77:**357–379. http://dx.doi.org/10.1128/MMBR.00061-12.
17. **Cheng S, Liu Y, Crowley CS, Yeates TO, Bobik TA.** 2008. Bacterial microcompartments: their properties and paradoxes. Bioessays **30:**1084–1095. http://dx.doi.org/10.1002/bies.20830.
18. **Yeates TO, Kerfeld CA, Heinhorst S, Cannon GC, Shively JM.** 2008. Protein-based organelles in bacteria: carboxysomes and related microcompartments. Nat. Rev. Microbiol. **6:**681–691. http://dx.doi.org/10.1038/nrmicro1913.
19. **Bobik TA.** 2007. Bacterial microcompartments. Microbe **2:**25–31. http://www.microbemagazine.org/images/stories/arch2007/jan07/znw00107000025.pdf.
20. **Abdul-Rahman F, Petit E, Blanchard JL.** 2013. The distribution of polyhedral bacterial microcompartments suggests frequent horizontal transfer and operon reassembly. J. Phylogenet. Evol. Biol. **1:**4. http://esciencecentral.org/journals/the-distribution-of-polyhedral-bacterial-microcompartments-suggests-frequent-horizontal-transfer-and-operon-reassembly-2329-9002.1000118.pdf.
21. **Penrod JT, Roth JR.** 2006. Conserving a volatile metabolite: a role for carboxysome-like organelles in *Salmonella enterica*. J. Bacteriol. **188:**2865–2874. http://dx.doi.org/10.1128/JB.188.8.2865-2874.2006.
22. **Havemann GD, Sampson EM, Bobik TA.** 2002. PduA is a shell protein of polyhedral organelles involved in coenzyme B_{12}-dependent degradation of 1,2-propanediol in *Salmonella enterica* serovar Typhimurium LT2. J. Bacteriol. **184:**1253–1261. http://dx.doi.org/10.1128/JB.184.5.1253-1261.2002.
23. **Rondon RR, Horswill AR, Escalante-Semerena JC.** 1995. DNA polymerase I function is required for the utilization of ethanolamine, 1,2-propanediol, and propionate by *Salmonella typhimurium* LT2. J. Bacteriol. **177:**7119–7124.
24. **Sampson EM, Bobik TA.** 2008. Microcompartments for B_{12}-dependent 1,2-propanediol degradation provide protection from DNA and cellular damage by a reactive metabolic intermediate. J. Bacteriol. **190:**2966–2971. http://dx.doi.org/10.1128/JB.01925-07.
25. **Dou Z, Heinhorst S, Williams EB, Murin CD, Shively JM, Cannon GC.** 2008. CO_2 fixation kinetics of *Halothiobacillus neapolitanus* mutant carboxysomes lacking carbonic anhydrase suggest the shell acts as a diffusional barrier for CO_2. J. Biol. Chem. **283:**10377–10384. http://dx.doi.org/10.1074/jbc.M709285200.
26. **Price GD, Badger MR.** 1989. Expression of human carbonic anhydrase in the cyanobacterium *Synechococcus* PCC7942 creates a high CO_2-requiring phenotype: evidence for a central role for carboxysomes in the CO_2 concentrating mechanism. Plant Physiol. **91:**505–513. http://dx.doi.org/10.1104/pp.91.2.505.
27. **Erbilgin O, McDonald KL, Kerfeld CA.** 2014. Characterization of a planctomycetal organelle: a novel bacterial microcompartment for the aerobic degradation of plant saccharides. Appl. Environ. Microbiol. **80:**2193–2205. http://dx.doi.org/10.1128/AEM.03887-13.
28. **Bobik TA, Xu Y, Jeter RM, Otto KE, Roth JR.** 1997. Propanediol utilization genes (*pdu*) of *Salmonella typhimurium*: three genes for the propanediol dehydratase. J. Bacteriol. **179:**6633–6639.
29. **Lawrence JG, Roth JR.** 1996. Evolution of coenzyme B_{12} synthesis among enteric bacteria: evidence for loss and reacquisition of a multigene complex. Genetics **142:**11–24.
30. **Thiennimitr P, Winter SE, Winter MG, Xavier MN, Tolstikov V, Huseby DL, Sterzenbach T, Tsolis RM, Roth JR, Baumler AJ.** 2011. Intestinal inflammation allows *Salmonella* to use ethanolamine to compete with the microbiota. Proc. Natl. Acad. Sci. U. S. A. **108:**17480–17485. http://dx.doi.org/10.1073/pnas.1107857108.
31. **Price GD, Badger MR, Woodger FJ, Long BM.** 2008. Advances in understanding the cyanobacterial CO_2-concentrating-mechanism (CCM): functional components, Ci transporters, diversity, genetic regulation and prospects for engineering into plants. J. Exp. Bot. **59:**1441–1461. http://dx.doi.org/10.1093/jxb/erm112.
32. **Winter SE, Baumler AJ.** 2011. A breathtaking feat: to compete with the gut microbiota, Salmonella drives its host to provide a respiratory electron acceptor. Gut Microbes **2:**58–60. http://dx.doi.org/10.4161/gmic.2.1.14911.
33. **Winter SE, Thiennimitr P, Winter MG, Butler BP, Huseby DL, Crawford RW, Russell JM, Bevins CL, Adams LG, Tsolis RM, Roth JR, Baumler AJ.** 2010. Gut inflammation provides a respiratory electron acceptor for *Salmonella*. Nature **467:**426–429. http://dx.doi.org/10.1038/nature09415.
34. **Conner CP, Heithoff DM, Julio SM, Sinsheimer RL, Mahan MJ.** 1998. Differential patterns of acquired virulence genes distinguish *Salmonella* strains. Proc. Natl. Acad. Sci. U. S. A. **95:**4641–4645. http://dx.doi.org/10.1073/pnas.95.8.4641.
35. **Heithoff DM, Conner CP, Hentschel U, Govantes F, Hanna PC, Mahan MJ.** 1999. Coordinate intracellular expression of *Salmonella* genes induced during infection. J. Bacteriol. **181:**799–807.
36. **Buchrieser C, Rusniok C, Kunst F, Cossart P, Glaser P.** 2003. Comparison of the genome sequences of *Listeria monocytogenes* and *Listeria innocua*: clues for evolution and pathogenicity. FEMS Immunol. Med. Microbiol. **35:**207–213. http://dx.doi.org/10.1016/S0928-8244(02)00448-0.
37. **Joseph B, Przybilla K, Stuhler C, Schauer K, Slaghuis J, Fuchs TM, Goebel W.** 2006. Identification of *Listeria monocytogenes* genes contributing to intracellular replication by expression profiling and mutant

screening. J. Bacteriol. **188:**556–568. http://dx.doi.org/10.1128/JB.188.2.556-568.2006.
38. **Price-Carter M, Tingey J, Bobik TA, Roth JR.** 2001. The alternative electron acceptor tetrathionate supports B_{12}-dependent anaerobic growth of *Salmonella enterica* serovar Typhimurium on ethanolamine or 1,2-propanediol. J. Bacteriol. **183:**2463–2475. http://dx.doi.org/10.1128/JB.183.8.2463-2475.2001.
39. **Fan C, Bobik TA.** 2011. The N-terminal region of the medium subunit (PduD) packages adenosylcobalamin-dependent diol dehydratase (PduCDE) into the Pdu microcompartment. J. Bacteriol. **193:**5623–5628. http://dx.doi.org/10.1128/JB.05661-11.
40. **Fan C, Cheng S, Liu Y, Escobar CM, Crowley CS, Jefferson RE, Yeates TO, Bobik TA.** 2010. Short N-terminal sequences package proteins into bacterial microcompartments. Proc. Natl. Acad. Sci. U. S. A. **107:**7509–7514. http://dx.doi.org/10.1073/pnas.0913199107.
41. **Fan C, Cheng S, Sinha S, Bobik TA.** 2012. Interactions between the termini of lumen enzymes and shell proteins mediate enzyme encapsulation into bacterial microcompartments. Proc. Natl. Acad. Sci. U. S. A. **109:**14995–15000. http://dx.doi.org/10.1073/pnas.1207516109.
42. **Choudhary S, Quin MB, Sanders MA, Johnson ET, Schmidt-Dannert C.** 2012. Engineered protein nano-compartments for targeted enzyme localization. PLoS One **7:**e33342. http://dx.doi.org/10.1371/journal.pone.0033342.
43. **Daniel R, Bobik TA, Gottschalk G.** 1998. Biochemistry of coenzyme B_{12}-dependent glycerol and diol dehydratases and organization of the encoding genes. FEMS Microbiol. Rev. **22:**553–566. http://dx.doi.org/10.1111/j.1574-6976.1998.tb00387.x.
44. **Tobimatsu T, Kawata M, Toraya T.** 2005. The N-terminal regions of beta and gamma subunits lower the solubility of adenosylcobalamin-dependent diol dehydratase. Biosci. Biotechnol. Biochem. **69:**455–462. http://dx.doi.org/10.1271/bbb.69.455.
45. **Sutter M, Boehringer D, Gutmann S, Gunther S, Prangishvili D, Loessner MJ, Stetter KO, Weber-Ban E, Ban N.** 2008. Structural basis of enzyme encapsulation into a bacterial nanocompartment. Nat. Struct. Mol. Biol. **15:**939–947. http://dx.doi.org/10.1038/nsmb.1473.
46. **Kinney JN, Salmeen A, Cai F, Kerfeld CA.** 2012. Elucidating essential role of conserved carboxysomal protein CcmN reveals common feature of bacterial microcompartment assembly. J. Biol. Chem. **287:**17729–17736. http://dx.doi.org/10.1074/jbc.M112.355305.
47. **Menon BB, Dou Z, Heinhorst S, Shively JM, Cannon GC.** 2008. *Halothiobacillus neapolitanus* carboxysomes sequester heterologous and chimeric RubisCO species. PLoS One **3:**e3570. http://dx.doi.org/10.1371/journal.pone.0003570.
48. **Parsons JB, Frank S, Bhella D, Liang M, Prentice MB, Mulvihill DP, Warren MJ.** 2010. Synthesis of empty bacterial microcompartments, directed organelle protein incorporation, and evidence of filament-associated organelle movement. Mol. Cell **38:**305–315. http://dx.doi.org/10.1016/j.molcel.2010.04.008.
49. **Kim EY, Tullman-Ercek D.** 2014. A rapid flow cytometry assay for the relative quantification of protein encapsulation into bacterial microcompartments. Biotechnol. J. **9:**348–354. http://dx.doi.org/10.1002/biot.201300391.
50. **Lawrence AD, Frank S, Newnham S, Lee MJ, Brown IR, Xue W-F, Rowe ML, Mulvihill DP, Prentice MB, Howard MJ, Warren MJ.** 30 January 2014. Solution structure of a bacterial microcompartment targeting peptide and its application in the construction of an ethanol bioreactor. ACS Synth. Biol. http://dx.doi.org/10.1021/sb4001118.
51. **Long BM, Rae BD, Badger MR, Price GD.** 2011. Over-expression of the beta-carboxysomal CcmM protein in *Synechococcus* PCC7942 reveals a tight co-regulation of carboxysomal carbonic anhydrase (CcaA) and M58 content. Photosynth. Res. **109:**33–45. http://dx.doi.org/10.1007/s11120-011-9659-8.
52. **Long BM, Tucker L, Badger MR, Price GD.** 2010. Functional cyanobacterial beta-carboxysomes have an absolute requirement for both long and short forms of the CcmM protein. Plant Physiol. **153:**285–293. http://dx.doi.org/10.1104/pp.110.154948.
53. **Long BM, Badger MR, Whitney SM, Price GD.** 2007. Analysis of carboxysomes from *Synechococcus* PCC7942 reveals multiple Rubisco complexes with carboxysomal proteins CcmM and CcaA. J. Biol. Chem. **282:**29323–29335. http://dx.doi.org/10.1074/jbc.M703896200.
54. **Long B, Badger M, Whitney S, Price D.** 2007. A structural role for CcmM in beta-carboxysome shell formation. Photosynth. Res. **91:**223.
55. **Cameron JC, Wilson SC, Bernstein SL, Kerfeld CA.** 2013. Biogenesis of a bacterial organelle: the carboxysome assembly pathway. Cell **155:**1131–1140. http://dx.doi.org/10.1016/j.cell.2013.10.044.
56. **Chen AH, Robinson-Mosher A, Savage DF, Silver PA, Polka JK.** 2013. The bacterial carbon-fixing organelle is formed by shell envelopment of preassembled cargo. PLoS One **8:**e76127. http://dx.doi.org/10.1371/journal.pone.0076127.
57. **Iancu CV, Morris DM, Dou Z, Heinhorst S, Cannon GC, Jensen GJ.** 2010. Organization, structure, and assembly of a-carboxysomes determined by electron cryotomography of intact cells. J. Mol. Biol. **396:**105–117. http://dx.doi.org/10.1016/j.jmb.2009.11.019.
58. **Cheng S, Sinha S, Fan C, Liu Y, Bobik TA.** 2011. Genetic analysis of the protein shell of the microcompartments involved in coenzyme B_{12}-dependent 1,2-propanediol degradation by *Salmonella*. J. Bacteriol. **193:**1385–1392. http://dx.doi.org/10.1128/JB.01473-10.
59. **Bonacci W, Teng PK, Afonso B, Niederholtmeyer H, Grob P, Silver PA, Savage DF.** 2012. Modularity of a carbon-fixing protein organelle. Proc. Natl. Acad. Sci. U. S. A. **109:**478–483. http://dx.doi.org/10.1073/pnas.1108557109.
60. **Parsons JB, Dinesh SD, Deery E, Leech HK, Brindley AA, Heldt D, Frank S, Smales CM, Lunsdorf H, Rambach A, Gass MH, Bleloch A, McClean KJ, Munro AW, Rigby SE, Warren MJ, Prentice MB.** 2008. Biochemical and structural insights into bacterial organelle form and biogenesis. J. Biol. Chem. **283:**14366–14375. http://dx.doi.org/10.1074/jbc.M709214200.
61. **Tanaka S, Sawaya MR, Phillips M, Yeates TO.** 2009. Insights from multiple structures of the shell proteins from the beta-carboxysome. Protein Sci. **18:**108–120. http://dx.doi.org/10.1002/pro.14.
62. **Tanaka S, Kerfeld CA, Sawaya MR, Cai F, Heinhorst S, Cannon GC, Yeates TO.** 2008. Atomic-level models of the bacterial carboxysome shell. Science **319:**1083–1086. http://dx.doi.org/10.1126/science.1151458.
63. **Kerfeld CA, Sawaya MR, Tanaka S, Nguyen CV, Phillips M, Beeby M, Yeates TO.** 2005. Protein structures forming the shell of primitive bacterial organelles. Science **309:**936–938. http://dx.doi.org/10.1126/science.1113397.
64. **Dryden KA, Crowley CS, Tanaka S, Yeates TO, Yeager M.** 2009. Two-dimensional crystals of carboxysome shell proteins recapitulate the hexagonal packing of three-dimensional crystals. Protein Sci. **18:**2629–2635. http://dx.doi.org/10.1002/pro.272.
65. **Sagermann M, Ohtaki A, Nikolakakis K.** 2009. Crystal structure of the EutL shell protein of the ethanolamine ammonia lyase microcompartment. Proc. Natl. Acad. Sci. U. S. A. **106:**8883–8887. http://dx.doi.org/10.1073/pnas.0902324106.
66. **Klein MG, Zwart P, Bagby SC, Cai F, Chisholm SW, Heinhorst S, Cannon GC, Kerfeld CA.** 2009. Identification and structural analysis of a novel carboxysome shell protein with implications for metabolite transport. J. Mol. Biol. **392:**319–333. http://dx.doi.org/10.1016/j.jmb.2009.03.056.
67. **Heldt D, Frank S, Seyedarabi A, Ladikis D, Parsons JB, Warren MJ, Pickersgill RW.** 2009. Structure of a trimeric bacterial microcompartment shell protein, EtuB, associated with ethanol utilization in *Clostridium kluyveri*. Biochem. J. **423:**199–207. http://dx.doi.org/10.1042/BJ20090780.
68. **Crowley CS, Cascio D, Sawaya MR, Kopstein JS, Bobik TA, Yeates TO.** 2010. Structural insight into the mechanisms of transport across the *Salmonella enterica* Pdu microcompartment shell. J. Biol. Chem. **285:**37838–37846. http://dx.doi.org/10.1074/jbc.M110.160580.
69. **Crowley CS, Sawaya MR, Bobik TA, Yeates TO.** 2008. Structure of the PduU shell protein from the Pdu microcompartment of Salmonella. Structure **16:**1324–1332. http://dx.doi.org/10.1016/j.str.2008.05.013.
70. **Cai F, Sutter M, Cameron JC, Stanley DN, Kinney JN, Kerfeld CA.** 2013. The structure of CcmP, a tandem bacterial microcompartment domain protein from the beta-carboxysome, forms a subcompartment within a microcompartment. J. Biol. Chem. **288:**16055–16063. http://dx.doi.org/10.1074/jbc.M113.456897.
71. **Samborska B, Kimber MS.** 2012. A dodecameric CcmK2 structure suggests beta-carboxysomal shell facets have a double-layered organization. Structure **20:**1353–1362. http://dx.doi.org/10.1016/j.str.2012.05.013.
72. **Price GD, Howitt SM, Harrison K, Badger MR.** 1993. Analysis of a genomic DNA region from the cyanobacterium *Synechococcus* sp. strain PCC7942 involved in carboxysome assembly and function. J. Bacteriol. **175:**2871–2879.
73. **Cai F, Menon BB, Cannon GC, Curry KJ, Shively JM, Heinhorst S.** 2009. The pentameric vertex proteins are necessary for the icosahedral

carboxysome shell to function as a CO_2 leakage barrier. PLoS One **4:**e7521. http://dx.doi.org/10.1371/journal.pone.0007521.
74. **Forouhar F, Kuzin A, Seetharaman J, Lee I, Zhou W, Abashidze M, Chen Y, Yong W, Janjua H, Fang Y, Wang D, Cunningham K, Xiao R, Acton TB, Pichersky E, Klessig DF, Porter CW, Montelione GT, Tong L.** 2007. Functional insights from structural genomics. J. Struct. Funct. Genomics **8:**37–44. http://dx.doi.org/10.1007/s10969-007-9018-3.
75. **Wheatley NM, Gidaniyan SD, Liu Y, Cascio D, Yeates TO.** 2013. Bacterial microcompartment shells of diverse functional types possess pentameric vertex proteins. Protein Sci. **22:**660–665. http://dx.doi.org/10.1002/pro.2246.
76. **Tanaka S, Sawaya MR, Yeates TO.** 2010. Structure and mechanisms of a protein-based organelle in *Escherichia coli*. Science **327:**81–84. http://dx.doi.org/10.1126/science.1179513.
77. **Pang A, Liang M, Prentice MB, Pickersgill RW.** 2012. Substrate channels revealed in the trimeric *Lactobacillus reuteri* bacterial microcompartment shell protein PduB. Acta Crystallogr. D Biol. Crystallogr. **68:**1642–1652. http://dx.doi.org/10.1107/S0907444912039315.
78. **Pang A, Warren MJ, Pickersgill RW.** 2011. Structure of PduT, a trimeric bacterial microcompartment protein with a 4Fe-4S cluster-binding site. Acta Crystallogr. D Biol. Crystallogr. **67:**91–96. http://dx.doi.org/10.1107/S0907444910050201.
79. **Cheng S, Fan C, Sinha S, Bobik TA.** 2012. The PduQ enzyme is an alcohol dehydrogenase used to recycle NAD^+ internally within the Pdu microcompartment of *Salmonella enterica*. PLoS One **7:**e47144. http://dx.doi.org/10.1371/journal.pone.0047144.
80. **Cheng S, Bobik TA.** 2010. Characterization of the PduS cobalamin reductase of *Salmonella enterica* and its role in the Pdu microcompartment. J. Bacteriol. **192:**5071–5080. http://dx.doi.org/10.1128/JB.00575-10.
81. **Huseby DL, Roth JR.** 2013. Evidence that a metabolic microcompartment contains and recycles private cofactor pools. J. Bacteriol. **195:**2864–2879. http://dx.doi.org/10.1128/JB.02179-12.
82. **Havemann GD, Bobik TA.** 2003. Protein content of polyhedral organelles involved in coenzyme B_{12}-dependent degradation of 1,2-propanediol in *Salmonella enterica* serovar Typhimurium LT2. J. Bacteriol. **185:**5086–5095. http://dx.doi.org/10.1128/JB.185.17.5086-5095.2003.
83. **Leal NA, Havemann GD, Bobik TA.** 2003. PduP is a coenzyme-A-acylating propionaldehyde dehydrogenase associated with the polyhedral bodies involved in B_{12}-dependent 1,2-propanediol degradation by *Salmonella enterica* serovar Typhimurium LT2. Arch. Microbiol. **180:**353–361. http://dx.doi.org/10.1007/s00203-003-0601-0.
84. **Sinha S, Cheng S, Fan C, Bobik TA.** 2012. The PduM protein is a structural component of the microcompartments involved in coenzyme B_{12}-dependent 1,2-propanediol degradation by *Salmonella enterica*. J. Bacteriol. **194:**1912–1918. http://dx.doi.org/10.1128/JB.06529-11.
85. **Toraya T, Honda S, Fukui S.** 1979. Fermentation of 1,2-propanediol with 1,2-ethanediol by some genera of *Enterobacteriaceae*, involving coenzyme B_{12}-dependent diol dehydratase. J. Bacteriol. **139:**39–47.
86. **Obradors N, Badia J, Baldoma L, Aguilar J.** 1988. Anaerobic metabolism of the L-rhamnose fermentation product 1,2-propanediol in *Salmonella typhimurium*. J. Bacteriol. **170:**2159–2162.
87. **Jeter RM.** 1990. Cobalamin-dependent 1,2-propanediol utilization by *Salmonella typhimurium*. J. Gen. Microbiol. **136:**887–896. http://dx.doi.org/10.1099/00221287-136-5-887.
88. **Roth JR, Lawrence JG, Bobik TA.** 1996. Cobalamin (coenzyme B_{12}): synthesis and biological significance. Annu. Rev. Microbiol. **50:**137–181. http://dx.doi.org/10.1146/annurev.micro.50.1.137.
89. **Liu Y, Leal NA, Sampson EM, Johnson CL, Havemann GD, Bobik TA.** 2007. PduL is an evolutionarily distinct phosphotransacylase involved in B_{12}-dependent 1,2-propanediol degradation by *Salmonella enterica* serovar Typhimurium LT2. J. Bacteriol. **189:**1589–1596. http://dx.doi.org/10.1128/JB.01151-06.
90. **Horswill AR, Escalante-Semerena JC.** 1997. Propionate catabolism in *Salmonella typhimurium* LT2: two divergently transcribed units comprise the *prp* locus at 8.5 centisomes, *prpR* encodes a member of the sigma-54 family of activators, and the *prpBCDE* genes constitute an operon. J. Bacteriol. **179:**928–940.
91. **Horswill AR, Escalante-Semerena JC.** 1999. *Salmonella typhimurium* LT2 catabolizes propionate via the 2-methylcitric acid cycle. J. Bacteriol. **181:**5615–5623.
92. **Palacios S, Starai VJ, Escalante-Semerena JC.** 2003. Propionyl coenzyme A is a common intermediate in the 1,2-propanediol and propionate catabolic pathways needed for expression of the *prpBCDE* operon during growth of *Salmonella enterica* on 1,2-propanediol. J. Bacteriol. **185:**2802–2810. http://dx.doi.org/10.1128/JB.185.9.2802-2810.2003.
93. **Jeter RM, Olivera BM, Roth JR.** 1984. *Salmonella typhimurium* synthesizes cobalamin (vitamin B_{12}) de novo under anaerobic growth conditions. J. Bacteriol. **159:**206–213.
94. **Chen P, Ailion M, Bobik T, Stormo G, Roth J.** 1995. Five promoters integrate control of the *cob*/*pdu* regulon in *Salmonella typhimurium*. J. Bacteriol. **177:**5401–5410.
95. **Bobik TA, Ailion M, Roth JR.** 1992. A single regulatory gene integrates control of vitamin B_{12} synthesis and propanediol degradation. J. Bacteriol. **174:**2253–2266.
96. **Rondon MR, Escalante-Semerena JC.** 1992. The *poc* locus is required for 1,2-propanediol-dependent transcription of the cobalamin biosynthetic (*cob*) and propanediol utilization (*pdu*) genes of *Salmonella typhimurium*. J. Bacteriol. **174:**2267–2272.
97. **Roth JR, Lawrence JG, Rubenfield M, Kieffer-Higgins S, Church GM.** 1993. Characterization of the cobalamin (vitamin B_{12}) biosynthetic genes of *Salmonella typhimurium*. J. Bacteriol. **175:**3303–3016.
98. **Andersson DI.** 1992. Involvement of the Arc system in redox regulation of the Cob operon in *Salmonella typhimurium*. Mol. Microbiol. **6:**1491–1494. http://dx.doi.org/10.1111/j.1365-2958.1992.tb00869.x.
99. **Rondon MR, Escalante-Semerena JC.** 1996. In vitro analysis of the interactions between the PocR regulatory protein and the promoter region of the cobalamin biosynthetic (*cob*) operon of *Salmonella typhimurium* LT2. J. Bacteriol. **178:**2196–2203.
100. **Ailion M, Bobik TA, Roth JR.** 1993. Two global regulatory systems (Crp and Arc) control the cobalamin/propanediol regulon of *Salmonella typhimurium*. J. Bacteriol. **175:**7200–7208.
101. **Escalante-Semerena JC, Roth JR.** 1987. Regulation of cobalamin biosynthetic operons in *Salmonella typhimurium*. J. Bacteriol. **169:**2251–2258.
102. **Rondon MR, Kazmierczak R, Escalante-Semerena JC.** 1995. Glutathione is required for maximal transcription of the cobalamin biosynthetic and 1,2-propanediol utilization (*cob/pdu*) regulon and for the catabolism of ethanolamine, 1,2-propanediol, and propionate in *Salmonella typhimurium* LT2. J. Bacteriol. **177:**5434–5439.
103. **Chang MC, Keasling JD.** 2006. Production of isoprenoid pharmaceuticals by engineered microbes. Nat. Chem. Biol. **2:**674–681. http://dx.doi.org/10.1038/nchembio836.
104. **Johnson CL, Buszko ML, Bobik TA.** 2004. Purification and initial characterization of the *Salmonella enterica* PduO ATP:cob(I)alamin adenosyltransferase. J. Bacteriol. **186:**7881–7887. http://dx.doi.org/10.1128/JB.186.23.7881-7887.2004.
105. **Johnson CL, Pechonick E, Park SD, Havemann GD, Leal NA, Bobik TA.** 2001. Functional genomic, biochemical, and genetic characterization of the *Salmonella pduO* gene, an ATP:cob(I)alamin adenosyltransferase gene. J. Bacteriol. **183:**1577–1584. http://dx.doi.org/10.1128/JB.183.5.1577-1584.2001.
106. **Parsons JB, Lawrence AD, McLean KJ, Munro AW, Rigby SE, Warren MJ.** 2010. Characterisation of PduS, the pdu metabolosome corrin reductase, and evidence of substructural organisation within the bacterial microcompartment. PLoS One **5:**e14009. http://dx.doi.org/10.1371/journal.pone.0014009.
107. **Sampson EM, Johnson CL, Bobik TA.** 2005. Biochemical evidence that the pduS gene encodes a bifunctional cobalamin reductase. Microbiology **151:**1169–1177. http://dx.doi.org/10.1099/mic.0.27755-0.
108. **Abeles RH, Lee HA, Jr.** 1961. An intramolecular oxidation-reduction requiring a cobamide coenzyme. J. Biol. Chem. **236:**2347–2350.
109. **Walter D, Ailion M, Roth J.** 1997. Genetic characterization of the *pdu* operon: use of 1,2-propanediol in *Salmonella typhimurium*. J. Bacteriol. **179:**1013–1022.
110. **Poznanskaja AA, Tanizawa K, Soda K, Toraya T, Fukui S.** 1979. Coenzyme B_{12}-dependent diol dehydrase: purification, subunit heterogeneity, and reversible association. Arch. Biochem. Biophys. **194:**379–386. http://dx.doi.org/10.1016/0003-9861(79)90630-1.
111. **Sauvageot N, Muller C, Hartke A, Auffray Y, Laplace J-M.** 2002. Characterisation of the diol dehydratase *pdu* operon of *Lactobacillus collinoides*. FEMS Microbiol. Lett. **209:**69–74. http://dx.doi.org/10.1016/S0378-1097(02)00471-8.
112. **Sauvageot N, Pichereau V, Louarme L, Hartke A, Auffray Y, Laplace JM.** 2002. Purification, characterization and subunits identification of the diol dehydratase of *Lactobacillus collinoides*. Eur. J. Biochem. **269:**5731–5737. http://dx.doi.org/10.1046/j.1432-1033.2002.03288.x.

113. **Tobimatsu T, Sakai T, Hashida Y, Mizoguchi N, Miyoshi S, Toraya T.** 1997. Heterologous expression, purification, and properties of diol dehydratase, an adenosylcobalamin-dependent enzyme of *Klebsiella oxytoca*. Arch. Biochem. Biophys. **347:**132–140. http://dx.doi.org/10.1006/abbi.1997.0325.
114. **Toraya T, Honda S, Mori K.** 2010. Coenzyme B12-dependent diol dehydratase is a potassium ion-requiring calcium metalloenzyme: evidence that the substrate-coordinated metal ion is calcium. Biochemistry **49:**7210–7217. http://dx.doi.org/10.1021/bi100561m.
115. **Shibata N, Masuda J, Tobimatsu T, Toraya T, Suto K, Morimoto Y, Yasuoka N.** 1999. A new mode of B_{12} binding and the direct participation of a potassium ion in enzyme catalysis: X-ray structure of diol dehydratase. Structure **7:**997–1008. http://dx.doi.org/10.1016/S0969-2126(99)80126-9.
116. **Luo LH, Kim CH, Heo SY, Oh BR, Hong WK, Kim S, Kim DH, Seo JW.** 2012. Production of 3-hydroxypropionic acid through propionaldehyde dehydrogenase PduP mediated biosynthetic pathway in *Klebsiella pneumoniae*. Bioresour. Technol. **103:**1–6. http://dx.doi.org/10.1016/j.biortech.2011.09.099.
117. **Luo LH, Seo JW, Baek JO, Oh BR, Heo SY, Hong WK, Kim DH, Kim CH.** 2011. Identification and characterization of the propanediol utilization protein PduP of *Lactobacillus reuteri* for 3-hydroxypropionic acid production from glycerol. Appl. Microbiol. Biotechnol. **89:**697–703. http://dx.doi.org/10.1007/s00253-010-2887-6.
118. **Tsang AW, Horswill AR, Escalante-Semerena JC.** 1998. Studies of regulation of expression of the propionate (*prpBCDE*) operon provide insights into how *Salmonella typhimurium* LT2 integrates its 1,2-propanediol and propionate catabolic pathways. J. Bacteriol. **180:**6511–6518.
119. **Honda S, Toraya T, Fukui S.** 1980. In situ reactivation of glycerol-inactivated coenzyme B_{12}-dependent enzymes, glycerol dehydratase and diol dehydratase. J. Bacteriol. **143:**1458–1465.
120. **Ushio K, Honda S, Toraya T, Fukui S.** 1982. The mechanism of in situ reactivation of glycerol-inactivated coenzyme B_{12}-dependent enzymes, glycerol dehydratase and diol dehydratase. J. Nutr. Sci. Vitaminol. (Tokyo) **28:**225–236. http://dx.doi.org/10.3177/jnsv.28.225.
121. **Toraya T.** 2000. Radical catalysis of B_{12} enzymes: structure, mechanism, inactivation, and reactivation of diol and glycerol dehydratases. Cell. Mol. Life Sci. **57:**106–127. http://dx.doi.org/10.1007/s000180050502.
122. **Mori K, Toraya T.** 1999. Mechanism of reactivation of coenzyme B_{12}-dependent diol dehydratase by a molecular chaperone-like reactivating factor. Biochemistry **38:**13170–13178. http://dx.doi.org/10.1021/bi9911738.
123. **Mori K, Tobimatsu T, Hara T, Toraya T.** 1997. Characterization, sequencing, and expression of the genes encoding a reactivating factor for glycerol-inactivated adenosylcobalamin-dependent diol dehydratase. J. Biol. Chem. **272:**32034–32041. http://dx.doi.org/10.1074/jbc.272.51.32034.
124. **Mori K, Tobimatsu T, Toraya T.** 1997. A protein factor is essential for in situ reactivation of glycerol-inactivated adenosylcobalamin-dependent diol dehydratase. Biosci. Biotechnol. Biochem. **61:**1729–1733. http://dx.doi.org/10.1271/bbb.61.1729.
125. **Tobimatsu T, Kajiura H, Yunoki M, Azuma M, Toraya T.** 1999. Identification and expression of the genes encoding a reactivating factor for adenosylcobalamin-dependent glycerol dehydratase. J. Bacteriol. **181:**4110–4113.
126. **Toraya T, Mori K.** 1999. A reactivating factor for coenzyme B_{12}-dependent diol dehydratase. J. Biol. Chem. **274:**3372–3377. http://dx.doi.org/10.1074/jbc.274.6.3372.
127. **Toraya T, Mori K, Hara T, Tobimatsu T.** 2000. A reactivating factor for coenzyme B_{12}-dependent diol dehydratase. Biofactors **11:**105–107. http://dx.doi.org/10.1002/biof.5520110131.
128. **Escalante-Semerena JC, Suh SJ, Roth JR.** 1990. *cobA* function is required for both de novo cobalamin biosynthesis and assimilation of exogenous corrinoids in *Salmonella typhimurium*. J. Bacteriol. **172:**273–280.
129. **Fonseca MV, Escalante-Semerena JC.** 2000. Reduction of cob(III)alamin to cob(II)alamin in *Salmonella enterica* serovar Typhimurium LT2. J. Bacteriol. **182:**4304–4309. http://dx.doi.org/10.1128/JB.182.15.4304-4309.2000.
130. **Fonseca MV, Escalante-Semerena JC.** 2001. An in vitro reducing system for the enzymic conversion of cobalamin to adenosylcobalamin. J. Biol. Chem. **276:**32101–32108. http://dx.doi.org/10.1074/jbc.M102510200.
131. **Pena KL, Castel SE, de Araujo C, Espie GS, Kimber MS.** 2010. Structural basis of the oxidative activation of the carboxysomal g-carbonic anhydrase, CcmM. Proc. Natl. Acad. Sci. U. S. A. **107:**2455–2460. http://dx.doi.org/10.1073/pnas.0910866107.
132. **Park K, Mera PE, Escalante-Semerena JC, Brunold TC.** 2008. Kinetic and spectroscopic studies of the ATP:corrinoid adenosyltransferase PduO from *Lactobacillus reuteri*: substrate specificity and insights into the mechanism of Co(II)corrinoid reduction. Biochemistry **47:**9007–9015. http://dx.doi.org/10.1021/bi800419e.
133. **St Maurice M, Mera PE, Taranto MP, Sesma F, Escalante-Semerena JC, Rayment I.** 2007. Structural characterization of the active site of the PduO-type ATP:co(I)rrinoid adenosyltransferase from *Lactobacillus reuteri*. J. Biol. Chem. **282:**2596–2605. http://dx.doi.org/10.1074/jbc.M609557200.
134. **Stich TA, Buan NR, Escalante-Semerena JC, Brunold TC.** 2005. Spectroscopic and computational studies of the ATP:corrinoid adenosyltransferase (CobA) from *Salmonella enterica*: insights into the mechanism of adenosylcobalamin biosynthesis. J. Am. Chem. Soc. **127:**8710–8719. http://dx.doi.org/10.1021/ja042142p.
135. **Stich TA, Yamanishi M, Banerjee R, Brunold TC.** 2005. Spectroscopic evidence for the formation of a four-coordinate Co^{2+} cobalamin species upon binding to the human ATP:cobalamin adenosyltransferase. J. Am. Chem. Soc. **127:**7660–7661. http://dx.doi.org/10.1021/ja050546r.
136. **Leal NA, Park SD, Kima PE, Bobik TA.** 2003. Identification of the human and bovine ATP:cob(I)alamin adenosyltransferase cDNAs based on complementation of a bacterial mutant. J. Biol. Chem. **278:**9227–9234. http://dx.doi.org/10.1074/jbc.M212739200.
137. **Dobson CM, Wai T, Leclerc D, Kadir H, Narang M, Lerner-Ellis JP, Hudson TJ, Rosenblatt DS, Gravel RA.** 2002. Identification of the gene responsible for the *cblB* complementation group of vitamin B_{12}-dependent methylmalonic aciduria. Hum. Mol. Genet. **11:**3361–3369. http://dx.doi.org/10.1093/hmg/11.26.3361.
138. **Zhang J, Dobson CM, Wu XC, Lerner-Ellis J, Rosenblatt DS, Gravel RA.** 2006. Impact of *cblB* mutations on the function of ATP:cob(I)alamin adenosyltransferase in disorders of vitamin B_{12} metabolism. Mol. Genet. Metab. **87:**315–322. http://dx.doi.org/10.1016/j.ymgme.2005.12.003.
139. **Mera PE, St Maurice M, Rayment I, Escalante-Semerena JC.** 2007. Structural and functional analyses of the human-type corrinoid adenosyltransferase (PduO) from *Lactobacillus reuteri*. Biochemistry **46:**13829–13836. http://dx.doi.org/10.1021/bi701622j.
140. **Saridakis V, Yakunin A, Xu X, Anandakumar P, Pennycooke M, Gu J, Cheung F, Lew JM, Sanishvili R, Joachimiak A, Arrowsmith CH, Christendat D, Edwards AM.** 2004. The structural basis for methylmalonic aciduria. The crystal structure of archaeal ATP:cobalamin adenosyltransferase. J. Biol. Chem. **279:**23646–23653. http://dx.doi.org/10.1074/jbc.M401395200.
141. **Mera PE, St Maurice M, Rayment I, Escalante-Semerena JC.** 2009. Residue Phe112 of the human-type corrinoid adenosyltransferase (PduO) enzyme of *Lactobacillus reuteri* is critical to the formation of the four-coordinate Co(II) corrinoid substrate and to the activity of the enzyme. Biochemistry **48:**3138–3145. http://dx.doi.org/10.1021/bi9000134.
142. **Toraya T, Shirakashi T, Kosuga T, Fukui S.** 1976. Substrate specificity of coenzyme B_{12}-dependent diol dehydrase: glycerol as both a good substrate and a potent inactivator. Biochem. Biophys. Res. Commun. **69:**475–480. http://dx.doi.org/10.1016/0006-291X(76)90546-5.
143. **Schneider Z, Pawelkiewicz J.** 1966. The properties of glycerol dehydratase isolated from *Aerobacter aerogenes*, and the properties of the apoenzyme subunits. Acta Biochim. Pol. **13:**311–328.
144. **Shibata N, Mori K, Hieda N, Higuchi Y, Yamanishi M, Toraya T.** 2005. Release of a damaged cofactor from a coenzyme B_{12}-dependent enzyme: X-ray structures of diol dehydratase-reactivating factor. Structure **13:**1745–1754. http://dx.doi.org/10.1016/j.str.2005.08.011.
145. **Laganowsky A, Liu C, Sawaya MR, Whitelegge JP, Park J, Zhao M, Pensalfini A, Soriaga AB, Landau M, Teng PK, Cascio D, Glabe C, Eisenberg D.** 2012. Atomic view of a toxic amyloid small oligomer. Science **335:**1228–1231. http://dx.doi.org/10.1126/science.1213151.
146. **Schulz GE.** 2002. The structure of bacterial outer membrane proteins. Biochim. Biophys. Acta **1565:**308–317. http://dx.doi.org/10.1016/S0005-2736(02)00577-1.
147. **Fan C, Bobik TA.** 2008. The PduX enzyme of *Salmonella enterica* is an

L-threonine kinase used for coenzyme B_{12} synthesis. J. Biol. Chem. **283:** 11322–11329. http://dx.doi.org/10.1074/jbc.M800287200.
148. **Fan C, Fromm HJ, Bobik TA.** 2009. Kinetic and functional analysis of L-threonine kinase, the PduX enzyme of *Salmonella enterica*. J. Biol. Chem. **284:**20240–20248. http://dx.doi.org/10.1074/jbc.M109.027425.
149. **Sriramulu DD, Liang M, Hernandez-Romero D, Raux-Deery E, Lunsdorf H, Parsons JB, Warren MJ, Prentice MB.** 2008. *Lactobacillus reuteri* DSM 20016 produces cobalamin-dependent diol dehydratase in metabolosomes and metabolizes 1,2-propanediol by disproportionation. J. Bacteriol. **190:**4559–4567. http://dx.doi.org/10.1128/JB.01535-07.
150. **Talarico TL, Axelsson LT, Novotny J, Fiuzat M, Dobrogosz WJ.** 1990. Utilization of glycerol as a hydrogen acceptor by *Lactobacillus reuteri*: purification of 1,3-propanediol:NAD oxidoreductase. Appl. Environ. Microbiol. **56:**943–948.
151. **Luthi-Peng Q, Dileme FB, Puhan Z.** 2002. Effect of glucose on glycerol bioconversion by *Lactobacillus reuteri*. Appl. Microbiol. Biotechnol. **59:** 289–296. http://dx.doi.org/10.1007/s00253-002-1002-z.
152. **Axelsson LT, Chung TC, Dobrogosz WJ, Lindgren SE.** 1989. Production of a broad spectrum antimicrobial substance by *Lactobacillus reuteri*. Microb. Ecol. Health Dis. **2:**131–136. http://dx.doi.org/10.3109/08910608909140210.
153. **Talarico TL, Casas IA, Chung TC, Dobrogosz WJ.** 1988. Production and isolation of reuterin, a growth inhibitor produced by *Lactobacillus reuteri*. Antimicrob. Agents Chemother. **32:**1854–1858. http://dx.doi.org/10.1128/AAC.32.12.1854.
154. **Morita H, Toh H, Fukuda S, Horikawa H, Oshima K, Suzuki T, Murakami M, Hisamatsu S, Kato Y, Takizawa T, Fukuoka H, Yoshimura T, Itoh K, O'Sullivan DJ, McKay LL, Ohno H, Kikuchi J, Masaoka T, Hattori M.** 2008. Comparative genome analysis of *Lactobacillus reuteri* and *Lactobacillus fermentum* reveal a genomic island for reuterin and cobalamin production. DNA Res. **15:**151–161. http://dx.doi.org/10.1093/dnares/dsn009.
155. **Bradbeer C.** 1965. The clostridial fermentations of choline and ethanolamine. II. Requirement for a cobamide coenzyme by an ethanolamine deaminase. J. Biol. Chem. **240:**4675–4681.
156. **Chang GW, Chang JT.** 1975. Evidence for the B_{12}-dependent enzyme ethanolamine deaminase in *Salmonella*. Nature **254:**150–151. http://dx.doi.org/10.1038/254150a0.
157. **Tsoy O, Ravcheev D, Mushegian A.** 2009. Comparative genomics of ethanolamine utilization. J. Bacteriol. **191:**7157–7164. http://dx.doi.org/10.1128/JB.00838-09.
158. **Shively JM, Bradburne CE, Aldrich HC, Bobik TA, Mehlman JL, Jin S, Baker SH.** 1998. Sequence homologs of the carboxysomal polypeptide CsoS1 of the thiobacilli are present in cyanobacteria and enteric bacteria that form carboxysomes-polyhedral bodies. Can. J. Bot. **76:**906–916. http://dx.doi.org/10.1139/b98-088.
159. **Garsin DA.** 2010. Ethanolamine utilization in bacterial pathogens: roles and regulation. Nat. Rev. Microbiol. **8:**290–295. http://dx.doi.org/10.1038/nrmicro2334.
160. **Roof DM, Roth JR.** 1988. Ethanolamine utilization in *Salmonella typhimurium*. J. Bacteriol. **170:**3855–3863.
161. **Roof DM, Roth JR.** 1989. Functions required for vitamin B_{12}-dependent ethanolamine utilization in *Salmonella typhimurium*. J. Bacteriol. **171:** 3316–3323.
162. **Mori K, Bando R, Hieda N, Toraya T.** 2004. Identification of a reactivating factor for adenosylcobalamin-dependent ethanolamine ammonia lyase. J. Bacteriol. **186:**6845–6854. http://dx.doi.org/10.1128/JB.186.20.6845-6854.2004.
163. **Buan NR, Escalante-Semerena JC.** 2006. Purification and initial biochemical characterization of ATP:cob(I)alamin adenosyltransferase (EutT) enzyme of *Salmonella enterica*. J. Biol. Chem. **281:**16971–16977. http://dx.doi.org/10.1074/jbc.M603069200.
164. **Buan NR, Suh SJ, Escalante-Semerena JC.** 2004. The *eutT* gene of *Salmonella enterica* encodes an oxygen-labile, metal-containing ATP: corrinoid adenosyltransferase enzyme. J. Bacteriol. **186:**5708–5714. http://dx.doi.org/10.1128/JB.186.17.5708-5714.2004.
165. **Sheppard DE, Penrod JT, Bobik T, Kofoid E, Roth JR.** 2004. Evidence that a B_{12}-adenosyl transferase is encoded within the ethanolamine operon of *Salmonella enterica*. J. Bacteriol. **186:**7635–7644. http://dx.doi.org/10.1128/JB.186.22.7635-7644.2004.
166. **Penrod JT, Mace CC, Roth JR.** 2004. A pH-sensitive function and phenotype: evidence that EutH facilitates diffusion of uncharged ethanolarnine in *Salmonella enterica*. J. Bacteriol. **186:**6885–6890. http://dx.doi.org/10.1128/JB.186.20.6885-6890.2004.
167. **Roof DM, Roth JR.** 1992. Autogenous regulation of ethanolamine utilization by a transcriptional activator of the *eut* operon in *Salmonella typhimurium*. J. Bacteriol. **174:**6634–6643.
168. **Sheppard DE, Roth JR.** 1994. A rationale for autoinduction of a transcriptional activator: ethanolamine ammonia-lyase (EutBC) and the operon activator (EutR) compete for adenosyl-cobalamin in *Salmonella typhimurium*. J. Bacteriol. **176:**1287–1296.
169. **Fox KA, Ramesh A, Stearns JE, Bourgogne A, Reyes-Jara A, Winkler WC, Garsin DA.** 2009. Multiple posttranscriptional regulatory mechanisms partner to control ethanolamine utilization in *Enterococcus faecalis*. Proc. Natl. Acad. Sci. U. S. A. **106:**4435–4440. http://dx.doi.org/10.1073/pnas.0812194106.
170. **Beeby M, Bobik TA, Yeates TO.** 2009. Exploiting genomic patterns to discover new supramolecular protein assemblies. Protein Sci. **18:**69–79. http://dx.doi.org/10.1002/pro.1.
171. **Scott KP, Martin JC, Campbell G, Mayer CD, Flint HJ.** 2006. Whole-genome transcription profiling reveals genes up-regulated by growth on fucose in the human gut bacterium "*Roseburia inulinivorans*." J. Bacteriol. **188:**4340–4349. http://dx.doi.org/10.1128/JB.00137-06.
172. **O'Brien JR, Raynaud C, Croux C, Girbal L, Soucaille P, Lanzilotta WN.** 2004. Insight into the mechanism of the B_{12}-independent glycerol dehydratase from *Clostridium butyricum*: preliminary biochemical and structural characterization. Biochemistry **43:**4635–4645. http://dx.doi.org/10.1021/bi035930k.
173. **Raynaud C, Sarcabal P, Meynial-Salles I, Croux C, Soucaille P.** 2003. Molecular characterization of the 1,3-propanediol (1,3-PD) operon of *Clostridium butyricum*. Proc. Natl. Acad. Sci. U. S. A. **100:**5010–5015. http://dx.doi.org/10.1073/pnas.0734105100.
174. **Petit E, LaTouf WG, Coppi MV, Warnick TA, Currie D, Romashko I, Deshpande S, Haas K, Alvelo-Maurosa JG, Wardman C, Schnell DJ, Leschine SB, Blanchard JL.** 2013. Involvement of a bacterial microcompartment in the metabolism of fucose and rhamnose by *Clostridium phytofermentans*. PLoS One **8:**e54337. http://dx.doi.org/10.1371/journal.pone.0054337.
175. **Seedorf H, Fricke WF, Veith B, Bruggemann H, Liesegang H, Strittmatter A, Miethke M, Buckel W, Hinderberger J, Li F, Hagemeier C, Thauer RK, Gottschalk G.** 2008. The genome of *Clostridium kluyveri*, a strict anaerobe with unique metabolic features. Proc. Natl. Acad. Sci. U. S. A. **105:**2128–2133. http://dx.doi.org/10.1073/pnas.0711093105.
176. **Hurtley S.** 2009. Spatial cell biology. Location, location, location. Introduction. Science **326:**1205. http://dx.doi.org/10.1126/science.326.5957.1205.
177. **Lopez-Gallego F, Schmidt-Dannert C.** 2010. Multi-enzymatic synthesis. Curr. Opin. Chem. Biol. **14:**174–183. http://dx.doi.org/10.1016/j.cbpa.2009.11.023.
178. **Held M, Quin MB, Schmidt-Dannert C.** 2013. Eut bacterial microcompartments: insights into their function, structure, and bioengineering applications. J. Mol. Microbiol. Biotechnol. **23:**308–320. http://dx.doi.org/10.1159/000351343.
179. **Chen AH, Silver PA.** 2012. Designing biological compartmentalization. Trends Cell Biol. **22:**662–670. http://dx.doi.org/10.1016/j.tcb.2012.07.002.
180. **Gehrmann W, Elsner M.** 2011. A specific fluorescence probe for hydrogen peroxide detection in peroxisomes. Free Radic. Res. **45:**501–516. http://dx.doi.org/10.3109/10715762.2011.560148.
181. **Moon TS, Dueber JE, Shiue E, Prather KL.** 2010. Use of modular, synthetic scaffolds for improved production of glucaric acid in engineered *E. coli*. Metab. Eng. **12:**298–305. http://dx.doi.org/10.1016/j.ymben.2010.01.003.
182. **Dueber JE, Wu GC, Malmirchegini GR, Moon TS, Petzold CJ, Ullal AV, Prather KL, Keasling JD.** 2009. Synthetic protein scaffolds provide modular control over metabolic flux. Nat. Biotechnol. **27:**753–759. http://dx.doi.org/10.1038/nbt.1557.
183. **Conrado RJ, Mansell TJ, Varner JD, DeLisa MP.** 2007. Stochastic reaction-diffusion simulation of enzyme compartmentalization reveals improved catalytic efficiency for a synthetic metabolic pathway. Metab. Eng. **9:**355–363. http://dx.doi.org/10.1016/j.ymben.2007.05.002.
184. **Kim EY, Tullman-Ercek D.** 2013. Engineering nanoscale protein compartments for synthetic organelles. Curr. Opin. Biotechnol. **24:**627–632. http://dx.doi.org/10.1016/j.copbio.2012.11.012.
185. **Worsdorfer B, Woycechowsky KJ, Hilvert D.** 2011. Directed evolution

of a protein container. Science **331:**589–592. http://dx.doi.org/10.1126/science.1199081.

186. **Chen HN, Woycechowsky KJ.** 2012. Conversion of a dodecahedral protein capsid into pentamers via minimal point mutations. Biochemistry **51:**4704–4712. http://dx.doi.org/10.1021/bi3003555.
187. **Lee H, DeLoache WC, Dueber JE.** 2012. Spatial organization of enzymes for metabolic engineering. Metab. Eng. **14:**242–251. http://dx.doi.org/10.1016/j.ymben.2011.09.003.
188. **Sargent F, Davidson FA, Kelly CL, Binny R, Christodoulides N, Gibson D, Johansson E, Kozyrska K, Lado LL, Maccallum J, Montague R, Ortmann B, Owen R, Coulthurst SJ, Dupuy L, Prescott AR, Palmer T.** 2013. A synthetic system for expression of components of a bacterial microcompartment. Microbiology **159:**2427–2436. http://dx.doi.org/10.1099/mic.0.069922-0.
189. **Lassila JK, Bernstein SL, Kinney JN, Axen SD, Kerfeld CA.** 11 March 2014. Assembly of robust bacterial microcompartment shells using building blocks from an organelle of unknown function. J. Mol. Biol. http://dx.doi.org/10.1016/j.jmb.2014.02.025.
190. **Tsai SJ, Yeates TO.** 2011. Bacterial microcompartments insights into the structure, mechanism, and engineering applications. Prog. Mol. Biol. Transl. Sci. **103:**1–20. http://dx.doi.org/10.1016/B978-0-12-415906-8.00008-X.